MergeMix: A Unified Augmentation Paradigm for Visual and Multi-Modal Understanding

Xin Jin[1,⋆] **Siyuan Li**[1,2,⋆] **Siyong Jian**[1] **Kai Yu**[1] **Huan Wang**[1,†]
[1]Westlake University, Hangzhou, China
[2]Zhejiang University, College of Computer Science and Technology, Hangzhou, China
{jinxin86; lisiyuan; wanghuan}@westlake.edu.cn
⋆ Equal contribution † Corresponding author
https://github.com/JinXins/MergeMix

arXiv:2510.23479v3 [cs.CV] 23 Feb 2026

Abstract

Vision-language alignment in multi-modal large language models (MLLMs) relies on supervised fine-tuning (SFT) or reinforcement learning (RL). To align multi-modal large language models (MLLMs) in the post-training stage, supervised fine-tuning (SFT) is a stable choice but requires human annotations and lacks task generalizations, while Reinforcement Learning (RL) searches for better answers from reward signals but suffers from computational overhead and instability. To achieve balance among scalability, efficiency, and alignment generalizations, we propose MergeMix, a unified paradigm that bridges SFT and RL with an efficient Token **Merge** based **Mix**up augmentation. As for the Mixup policy, we generate contextual aligned mixed images with the corresponding labels according to the merged attention maps with cluster regions. Then, we enhance the preference-driven paradigm for MLLMs by building preference pairs with raw images and MergeMix-generated ones and optimizing the soft preference margin with the mixed SimPO loss. Extensive experiments demonstrate that MergeMix not only achieves dominant classification accuracy as an augmentation method but also improves generalization abilities and alignment of MLLMs, providing a new learning paradigm for preference alignment with training efficiency and stability.

1 Introduction

Multi-modal Large Language Models (MLLMs) (Liu et al., 2024b; Bai et al., 2025; Tong et al., 2024) have recently demonstrated remarkable capabilities in integrating visual and textual information, enabling a wide range of applications from visual question answering to multi-modal reasoning. Since MLLMs are typically pre-trained on massive web-scale datasets, forcing them to possess a wide range of knowledge and general reasoning capabilities, Supervised Fine-Tuning (SFT) and Reinforcement Learning (RL)-based preference optimization (Yang et al., 2025c) have emerged as two primary paradigms for aligning MLLMs with human preferences and specific task requirements. However, SFT depends on high-quality instruction–response annotations and optimizes the likelihood of reference responses, which does not explicitly model relative preferences between outputs. RL-based methods such as RLHF are more preference-aware, but require an additional reward model that may introduce bias or be exploited by the reward signal.

Due to the shortcomings of data quality and training efficiency, some works (Zhu et al., 2024; 2025b; Luo et al., 2024; Tan et al., 2025; Wang et al., 2024b) try to build performance pairs for optimization. How to build the preference pair with control and high-quality data for model training is the remaining open question. For example, SeVa (Zhu et al., 2024) proposed a preference optimization method by building a loser through some classic augmentation (*i.e.*, RandomCrop). Then, select the different responses for optimizing the model by a DPO loss (Rafailov et al., 2023). However, these methods have two drawbacks: the augmentations are highly random, and the DPO loss cannot be related to the data, which means SeVa can only select useful training data. Those technical causes SeVa can not control the quality of the loser, which is harmful for some visual question answering tasks, and reduces the training data by selecting "hard negatives". Hence, we investigate an inter-

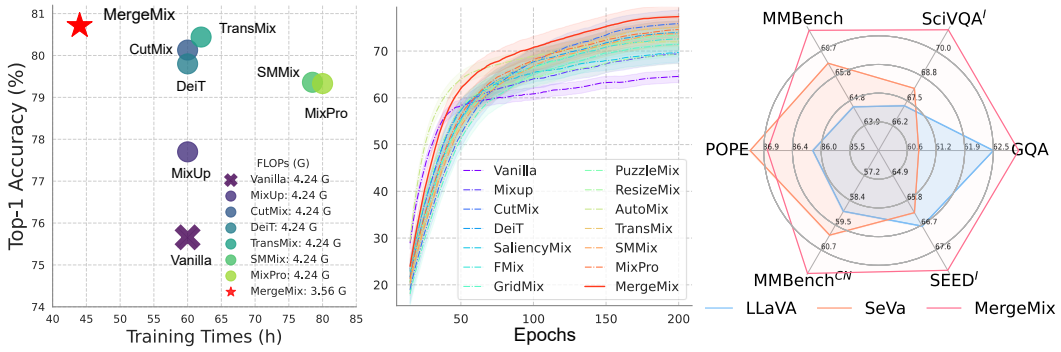

(a) Training Time vs. Accuracy (b) Epochs vs. Accuracy (c) LLaVA Benchmark

Figure 1: **Efficiency and performance for MergeMix.** (a) The training time *vs.* accuracy of mixup methods with the DeiT-Small model. (b) The image classification Top-1 accuracy *vs.* training epochs of different mixup methods on the CIFAR100 dataset with the DeiT-Tiny model. (c) The radar plot of the results on part VQA tasks by LLaVA-7B, LLaVA with SFT, and MergeMix.

esting question: *Is it necessary to propose novel techniques rather than some classical machine learning methods in the MLLM scenario?*

In this paper, we revisit the mixup augmentation, which synthesizes mixed samples and corresponding labels with given mixing ratios. However, two main challenges arise as illustrated in Figure 1: (1) achieving an optimal trade-off between efficiency and performance of mixup augmentations that rely on saliency-based metrics, (2) extending the augmentation to MLLMs properly, from classical image corruptions to data-dependent samples. Motivated by these perspectives, we propose a novel training framework called **MergeMix**, which builds preference pairs for MLLM training through data augmentation methods and ranking loss, thereby bridging the gap between SFT and RL. Figure 2 shows the two scenarios of MergeMix. **(a)** We introduce MergeMix, a novel data augmentation that generates mixed samples through token merge techniques. A bipartite soft matching strategy captures similarity information that preserves contextual features, ensuring the mask retains useful information. Meanwhile, MergeMix links the merge ratio and mixing ratio, aligning mixed images with the corresponding labels, enabling precise mixing data generation. **(b)** We propose a preference-driven paradigm for MLLMs, where augmented samples are defined as non-preferred responses (Loser) and clean samples as preferred responses (Winner). This paradigm facilitates preference tuning via the mixed SimPO loss, and leverages the mixing ratio as the soft preference margin to enable adaptive optimization. Altogether, Figure 1 shows these contributions yield an efficient and effective training strategy that achieves stronger alignment with human preferences while preserving the stability and scalability of SFT. Since the optimization object has a direct relationship with augmentation, it obtains a more robust ability in calibration. Extensive experiments show that MergeMix, as a training-time augmentation paradigm, achieves competitive performance in both image classification and MLLM benchmark with favorable efficiency.

Our contributions can be summarized as:

(a) We use token merging to obtain a local clustered attention map, enabling the generation of mixed images with cluster regions, a label re-scaling strategy aligned the mixed images with their corresponding labels, achieve well performance on both overhead and classification accuracy.

(b) We enhance the preference tuning paradigm for supervised fine-tuning of MLLMs, where mixed images are treated as losers, the mixing ratio is used as a soft preference reward score, and optimize the model adaptively via the mixed SimPO loss.

(c) We validate that our method achieves state-of-the-art on several image classification datasets and benchmarks, along with the advantages of our training paradigm on several MLLM benchmarks.

2 Related Work

In this section, we introduce the existing mixup approaches for image classification and token compression approaches in multi-modal large language models for efficient training or inference.

Mixup Augmentations The Mixup method mitigates model overfitting by generating augmented samples through mixing two different images within a mini-batch. Broadly, Mixup methods can be categorized into two types: **Static**, which relies on human priors or randomness, and **Adaptive**, a data-dependent type that leverages certain metrics to guide the mixing process. **(i) Static:** MixUp (Zhang et al., 2017) generates mixed samples via linear interpolation with λ. CutMix (Yun et al., 2019) extends this idea from the global pixel level to a local patch level by constructing a mask of size proportional to λ to mix images. ResizeMix (Qin et al., 2020) ensures that features from at least one class are always preserved in the mixed sample by resizing the source image before mixing. Other methods, *e.g.*, FMix (Harris et al., 2020), SmoothMix (Lee et al., 2020), GridMix (Baek et al., 2021), and StarMix (Jin et al., 2024b), focus on improving the mask to obtain more suitable mixed samples. **(ii) Adaptive:** SaliencyMix (Uddin et al., 2021) employs a saliency extractor to identify informative patches in images for mixing. Attentive-CutMix (Walawalkar et al., 2020) and SuperMix (Dabouei et al., 2021) utilize a teacher model to guide mask generation. PuzzleMix (Kim et al., 2020) and Co-Mix (Kim et al., 2021) generate appropriate masks based on gradient information obtained from a forward pass of the samples. AutoMix (Liu et al., 2022) and AdAutoMix (Qin et al., 2024a) adopt an end-to-end bi-optimization paradigm to produce mixed samples. TransMix (Chen et al., 2022), SMMix (Chen et al., 2023), and MixPro (Zhao et al., 2023) specifically enhance ViTs by computing attention scores from a forward pass to generate feature-aware masks and further refine the label ratio through attention scores. DiffuseMix (Islam et al., 2024a) and GenMix (Islam et al., 2024b) generate mixed samples by a diffusion model (Zhu et al., 2025a) for label preserving.

Token Compression in MLLMs Token compression methods (Bolya et al., 2023; Tao et al., 2025a; Shao et al., 2025; Chen et al., 2025; Tao et al., 2025b) mainly propose to merge or drop redundant tokens to achieve efficiency and acceleration. In MLLMs, images and texts will incur a significant number of tokens, which are often full of redundant information. Obvious researchers bring the token compression into MLLMs. Overall, we divide the methods that reduce tokens into 2 types, **Reduce in Encoder** and **Reduce in Decoder**. **(i) Reduce in Encoder:** MADTP (Cao et al., 2024) aims to achieve MLLM acceleration by purging visual tokens. LLaVA-PruMerge (Shang et al., 2024) uses the attention of `[CLS]` token to select clustering centers and then merges the remaining tokens with lower attention through a KNN clustering and weighted clustering center updating mechanism. VisionZip (Yang et al., 2025b), instead, retains visual tokens with high attention scores and subsequently merges the remaining tokens through clustering. Others, such as TokenPacker (Li et al., 2025), AVG-LLaVA (Lan et al., 2025), MustDrop (Liu et al., 2024c), and LLaVolta (Chen et al., 2024a), achieve acceleration by choosing a metric to sample TopK visual tokens. FastVLM (Vasu et al., 2025) proposes an Efficient Vision Encoder to reduce visual tokens. **(ii) Reduce in Deocder:** PyramidDrop (Xing et al., 2024) divides the token compression process in LLM into multiple stages, which employs a pyramidal token drop to avoid losing too much visual information in shallower layers. ATP-LLaVA (Ye et al., 2025) proposes an Adaptive Token Pruning (ATP) module that reduces the number of tokens in the decoder layer. ZipVL (He et al., 2024) proposes a dynamic ratio allocation strategy via the importance token, adaptively determined based on the distribution of attention scores in a particular layer, rather than a fixed hyperparameter.

3 PRELIMINARIES

Reformulation of Mixup Augmentation. We define $\mathbb{X}$ to be the set of training samples and $\mathbb{Y}$ the set of ground truth of the corresponding labels. For each sample pair (x, y), we randomly sample two pairs in $\mathbb{X}$ and $\mathbb{Y}$, with λ in Beta(α, α). The mixed images and labels are generated by applying the optimized mask $\mathcal{M}$ and ratio $\hat{\lambda}$, which come from a defined policy $\mathcal{P}(\cdot, \cdot, \cdot)$ according to Eq. (1):

$$\mathcal{M},\ \hat{\lambda} = \mathcal{P}\big(f_\theta(x_i, x_j),\ (y_i, y_j),\ \lambda\big), \tag{1}$$

$$\begin{aligned} \hat{x} &= \mathcal{M} \odot x_i + (1 - \mathcal{M}) \odot x_j, \\ \hat{y} &= \hat{\lambda} * y_i + (1 - \hat{\lambda}) * y_j, \end{aligned} \tag{2}$$

where the $\odot$ denotes element-wise multiplication. Policy $\mathcal{P}(\cdot, \cdot, \cdot)$ aims for the $\mathcal{M}$ to retain more features in the mixed sample. The $\hat{\lambda}$ keeps the initial sampling ratio when without optimization; otherwise, the λ can be re-computed by some metrics (*i.e.*, MergeMix uses the total mask values).

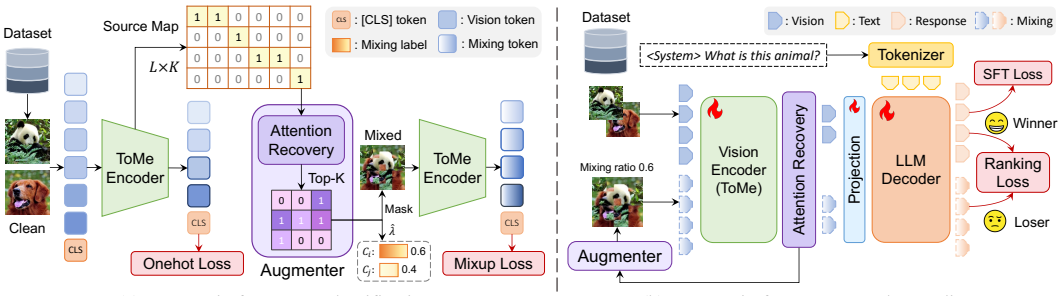

(a) MergeMix for Image Classification (b) MergeMix for MLLM Understanding

Figure 2: **Overview of MergeMix in two scenarios. (a) MergeMix for Image Classification:** The image is processed by the ToMe encoder, with Attention Score Recovery and TopK sampling to generate the corresponding class prediction. **(b) MergeMix for MLLM:** Preference pairs are encoded by the vision model with token merging, and the LLM decoder generates response text for the loser and winner, optimized via a ranking loss.

Preference Tuning for MLLMs. Preference optimization methods aim to align LLMs and MLLMs with human feedback by contrasting preferred and dispreferred responses. A general preference loss can be abstractly defined as Eq. (3):

$$\mathcal{L}_{\text{Pref}} = -\log \sigma\big(\pi_\theta(x, y^+) - \pi_\theta(x, y^-)\big), \tag{3}$$

where (x, y^+) and (x, y^-) denote the preferred and dispreferred responses respectively, and s_θ is a scoring function that reflects model preference. Different approaches (*e.g.*, PPO (Schulman et al., 2017), DPO (Rafailov et al., 2023)) instantiate π_θ in various ways, but all share the same principle.

Unlike RL-based approaches, which require training a separate reward model, DPO provides a simple and stable alternative by directly optimizing the policy model using preference pairs. Formally, the DPO loss is defined as Eq. (4):

$$\mathcal{L}_{\text{DPO}} = -\mathbb{E}(x, y^+, y^-) \sim \mathcal{D}\Big[\log \sigma\big(\beta \log \frac{\pi_\theta(y^+|x)}{\pi_{\text{ref}}(y^+|x)} - \beta \log \frac{\pi_\theta(y^-|x)}{\pi_{\text{ref}}(y^-|x)}\big)\Big], \tag{4}$$

where π_θ denotes the policy model (in our case, an MLLM such as LLaVA-v1.5 (Liu et al., 2024b) or Qwen-VL (Bai et al., 2025)), and π_{ref} represents a frozen reference model used to preserve alignment with the original pre-trained distribution. σ is the sigmoid function, and $\beta > 0$ is a temperature-like scaling factor that controls the sharpness of preference separation. Intuitively, DPO encourages the policy to assign a higher likelihood to preferred responses (y^+) than to non-preferred ones (y^-), while maintaining proximity to the reference model.

4 MergeMix Training Paradigm

In this section, we present the implementation of MergeMix, an augmentation approach via token merging for image mixing, not only for image classification, but also designed for multi-modal large language models. Figure 3 shows the overall pipeline of MergeMix, and we describe in two subsections in detail, which are from the input space to the loss objective for model training.

4.1 Image Mixing via Token Merge

In MergeMix, we leverage the relationship between the merge ratio and mixing ratio. The merge ratio measures the information of raw samples, while the mixing ratio balances the information between mixing samples, thereby enabling precise data generation of mixed inputs and labels. In this subsection, we first introduce MergeMix on the input space. Then we use the designed mixing policy $\mathcal{P}(\cdot, \cdot, \cdot)$ to obtain the mixed images $\hat{x}$ with the mask $\mathcal{M}$.

Image Policy with Token Merging. Unlike other mixup methods (Chen et al., 2022; 2023; Zhao et al., 2023), we introduce a ViT-based model $f_\theta(\cdot)$ iteratively replace N attention layers with ToMeAttention as ToMe (Bolya et al., 2023), Given the initial sequence $Z_L = f_\theta(\hat{x})$, then merges tokens as Eq. (5):

$$S, A_K, Z_K = \text{ToMeAttention}(Z_L, r), \tag{5}$$

where A_K denotes the attention map from the model, and Z_K denotes the feature tokens for computing one-hot loss. r denotes the number of merged tokens, which can reduce some high-similarity semantic tokens and retain a condensed token sequence. Also, based on Token Merge, we obtained a source map S for their spatial relationships between the raw token sequence Z_L and the Z_K.

Generating Mixing Mask with Source Matrix. Since token merging aggregates non-similar tokens into compact representations Z_K, the resulting matrix preserves local feature structures more effectively. In contrast, the vanilla TopK selection adopts a greedy sampling strategy with linear complexity $\mathcal{O}(N)$, which discards low-ranked tokens directly and thus loses spatial relationships. Alternatively, the Bipartite Soft Matching (BSM) approach performs global pairwise matching with quadratic complexity, yielding a more balanced and globally optimal merging of tokens. To reconstruct the full-resolution attention map, we introduce a recovering function $\mathcal{R}_{K\to L}(\cdot,\cdot)$ that expands the merged attention map A_K back to its original length A_L, which shows in Figure 5 and according to Eq. (6):

$$\hat{A_L} = \mathcal{R}_{K\to L}(A_K, S). \tag{6}$$

Unlike discrete TopK sampling, our recovery mechanism propagates merged attention over the original token topology guided by similarity S, restoring richer spatial dependencies and contextual continuity, thus reducing information loss from hard selection. Based on the encoder with a token merge and attention recovery. We can generate the binary $\mathcal{M}$ according to Eq. (7):

$$\mathcal{M}_i = \begin{cases} 1, & \text{if } i \in \text{TopK}(\hat{A}_L, p), \\ 0, & \text{otherwise}, \end{cases} \tag{7}$$

where p denotes the selection number, $p = \lfloor \lambda * L \rfloor$, and i denotes the index of sequence. Finally, we can mix the mini-batch and get the augmented data for $f_\theta(\cdot)$ training.

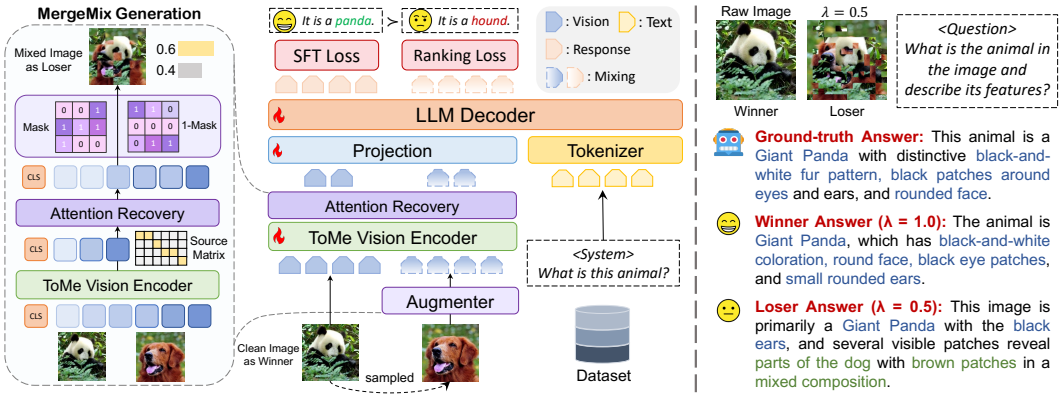

(a) MergeMix for MLLM Understanding (b) Case study of Preference Optimization

Figure 3: **Overall illustration of MergeMix for MLLM. (a)** MergeMix performs attention-based mask mixing guided by the ToMe Vision Encoder, recovering token attention scores and generating a mixed image through an augmenter. Specifically, Token Merging hierarchically merges visual tokens via Bipartite Soft Matching (BSM) to enhance efficiency, which is trained with both the SFT and ranking losses. **(b)** Case study of preference data generated by MergeMix with LLaVA-v1.5-7B.

4.2 A Unified Augmentation Paradigm: From Image Classification to MLLMs

In this subsection, we describe the loss function $\mathcal{L}$. For the classification task and visual understanding, our final loss $\mathcal{L}_{\text{Total}}$ combines two losses: the main loss (one-hot cross entropy loss $\mathcal{L}_{\text{CE}}$ and $\mathcal{L}_{\text{SFT}}$) and the reformulated loss (mixup cross entropy loss $\mathcal{L}_{\text{MCE}}$ and ranking loss $\mathcal{L}_{\text{SimPO}}^{\text{Mix}}$). Figure 3 shows the pipeline of MergeMix for MLLM in detail.

Re-scaling Policy for Mixing Ratio. Under this optimization objective, the role of the mixing ratio λ is to serve as a metric that quantifies the presence of feature information from the two samples. While this metric cannot directly reflect the true characteristics of the data, certain adaptive methods can constrain the model to generate mixed samples where the mixing ratio progressively approximates the target value (Jin et al., 2024a). Some works, like LUMix (Sun et al., 2022), DecoupleMix (Liu et al., 2023), and SUMix (Qin et al., 2024b), use a defined policy for some hand-crafted mixup methods, and find that it is more efficient than optimizing a better mask way.

Since we introduce a token-merging technology that inherently enables information aggregation and selection, the entire model training process must consider not only simple spatial ratios but also the degree of information integration within the model. So, we proposed a Gaussian-based sampling to refine the ratio, where the merged tokens and the mask values jointly control the `mean` and `std` as `mean`$= \frac{K}{L}$, and `std`$= \frac{p}{\sum_i^L \mathcal{M}}$. This smooth transition directly alleviates changes from linear mapping and yields more robust augmentations, with its formulation given as:

$$\hat{\lambda} \sim \mathcal{N}(\mu, \sigma), \quad \hat{\lambda} = \text{clip}\Big(\frac{\hat{\lambda} - \min(\hat{\lambda})}{\max(\hat{\lambda}) - \min(\hat{\lambda}) + \tau}, 0, 1\Big), \tag{8}$$

where the $\mathcal{N}(\cdot, \cdot)$ denotes a Gaussian function, μ and σ represent the merged ratio and mixing ratio repetitively. τ as a hyperparameter, set to `1e-5`. Then, we obtain the re-scaled mixing ratio $\hat{\lambda}$ with spatial and ToMe model inherent features to optimize the model when training. In total, the loss of mixup training as:

$$\mathcal{L}_{\text{Total}} = \underbrace{\mathcal{L}_{\text{CE}}\big(f_\theta(\hat{x}), y_i\big) * \hat{\lambda} + \mathcal{L}_{\text{CE}}\big(f_\theta(\hat{x}), y_j\big) * (1 - \hat{\lambda})}_{\text{mce loss}} + \underbrace{\mathcal{L}_{\text{CE}}\big(f_\theta(x), y\big)}_{\text{one-hot loss}}. \tag{9}$$

Aggregating Mixing Ratio within Preference Loss. LLaVA (Liu et al., 2024b) uses a standard conditional language modeling loss for SFT. In MLLMs, we are given an instruction–response pair (x, y), where x denotes the multi-modal data, inducing vision and text, and $y = (y_1, y_{|y|})$ denotes the target response. The SFT loss is defined as:

$$\mathcal{L}_{\text{SFT}} = -\mathbb{E}_{(x,y)\sim\mathcal{D}}\left[\sum_{t=1}^{|y|} \log \pi_\theta\big(y_t \mid x, y_{<t}\big)\right]. \tag{10}$$

This objective needs to maximize the likelihood of GT responses, aiming to align the data. In Section 3, we introduced the DPO loss, which can be decomposed into two components: the SFT part and the ranking optimization part. In our approach, we replace the ranking component with SimPO (Meng et al., 2024), where y denotes the target sequence (response) and $|y|$ denotes its length. Furthermore, since λ reflects information similarity between augmented and raw image (interpreted as "loser degree" in MLLMs), we link it to $\gamma \rightarrow 1 - \hat{\lambda}$: larger λ represent higher similarity and harder discrimination, reduces γ to avoid over-optimization on trivial differences; smaller λ represent greater dissimilarity and easier tasks increases γ to strengthen constraints for clearer preference distinction. The mixed SimPO loss replacement is Eq. (11):

$$\mathcal{L}_{\text{SimPO}}^{\text{Mix}} = -\mathbb{E}_{(x,\hat{x},y)\sim\mathcal{D}}\Big[\log \sigma\big(\frac{\beta}{|y|}\log \pi_\theta(y \mid x) - \frac{\beta}{|y|}\log \pi_\theta(y \mid \hat{x}) - (1 - \hat{\lambda})\big)\Big]. \tag{11}$$

This reformulated loss strictness with sample difficulty, enabling more robust preference optimization. Finally, the total loss of our training paradigm is written as:

$$\mathcal{L}_{\text{Total}} = \mathcal{L}_{\text{SFT}} + \mathcal{L}_{\text{SimPO}}^{\text{Mix}}. \tag{12}$$

5 Experiments

5.1 State-of-the-art methods

Image classification. To evaluate the performance of MergeMix, we compared with some mainstream mixup methods, *i.e.* Mixup (Zhang et al., 2017), CutMix (Yun et al., 2019), FMix (Harris et al., 2020), SmoothMix (Lee et al., 2020), GridMix (Baek et al., 2021), ResizeMix (Qin et al., 2020), SaliencyMix (Uddin et al., 2021), Attentive-CutMix (Walawalkar et al., 2020), PuzzleMix (Kim et al., 2020), GuidedMixup (Kang & Kim, 2023), AutoMix (Liu et al., 2022) and AdAutoMix (Qin et al., 2024a). DeiT (Touvron et al., 2021), TransMix (Chen et al., 2022), SMMix (Chen et al., 2023), MixPro (Zhao et al., 2023) and TdAttenMix (Wang et al., 2025) for some ViT-based methods. The training configures about datasets and methods follows the open-source library OpenMixup (Li et al., 2022).

Table 1: Top-1 accuracy (%) of mixup methods training 200 epochs on CIFAR100 dataset with different model sizes. T/S/B/L denotes Tiny, Small, Base, and Large, respectively. The full results of training 600 epochs are in Table A1.

Method	DeiT-T	DeiT-S	ViT-S	ViT-B	ViT-L
Vanilla	64.70	65.81	62.64	63.33	61.83
MixUp	69.47	69.98	68.67	69.66	67.90
CutMix	75.98	74.21	69.67	72.18	68.97
FMix	72.73	70.41	68.41	68.62	66.12
GridMix	71.54	68.86	70.15	66.63	63.20
ResizeMix	69.42	68.54	67.86	63.72	63.48
SaliencyMix	69.83	69.78	70.14	68.75	67.12
PuzzleMix	73.40	73.60	70.92	71.13	69.77
AutoMix	72.91	76.24	68.44	73.40	72.10
AdAutoMix	72.83	72.63	69.66	71.43	69.69
DeiT	74.01	75.92	72.96	72.15	69.23
TransMix	75.31	76.17	74.15	72.87	71.40
SMMix	73.84	74.09	73.50	70.87	71.38
MixPro	74.78	75.26	73.49	73.18	72.28
TdAttenMix	73.63	73.32	73.11	72.19	72.12
MergeMix	**77.46**	**78.68**	**77.02**	**75.75**	**76.19**

Table 2: Top-1 accuracy (%) of mixup methods on the Stanford-Cars dataset. Full results of the CUB200 and FGVC-Aircrafts dataset in Table A2.

Method	α	DeiT-S	ViT-B
Vanilla	–	86.77	91.31
MixUp	1.0	87.73	91.36
CutMix	0.2	88.37	91.53
SmoothMix	0.2	86.39	90.88
FMix	0.2	87.18	91.36
GridMix	0.2	87.58	91.31
ResizeMix	1.0	87.45	91.59
Attentive-CutMix	2.0	87.35	90.29
SaliencyMix	0.2	87.94	91.47
PuzzleMix	1.0	88.60	91.83
GuidedMix^{ap}	1.0	86.99	90.40
DeiT	0.2	88.72	92.17
TransMix	1.0	88.38	91.66
SMMix	1.0	88.76	91.93
MixPro	1.0	88.38	91.48
TdAttenMix	1.0	88.78	91.68
MergeMix	1.0	**89.42**	**92.20**

MLLMs. To evaluate the training paradigm that we proposed, we compare with three different system-level baselines: **(1)** SFT with different training paradigms on LLaVA, including LLaVA-NeXT-7/13B (Liu et al., 2024a), SeVa-7B (Zhu et al., 2024), SIMA (Wang et al., 2024b), and nSFT (Zhu et al., 2025b). **(2).** Token reduction on LLaVA, including LLaVA-PruMerge+ (Shang et al., 2024), VisionZip (Yang et al., 2025b), VisPrunner (Zhang et al., 2024b), VScan (Zhang et al., 2025a), and LLaVA-Mini (Zhang et al., 2025b). **(3).** RL training on Qwen2.5-VL-Instruction (Bai et al., 2025), including VisionThink (Yang et al., 2025c).

For all classification results, we report the top-1 test accuracy in the last 10 training epochs for each trial. To facilitate comparison, we mark the best and second best results in **bold** and cyan. For the LLaVA benchmark, we use the LLaVA official code, and for the Qwen2.5-VL-Instruction benchmark. We use lmms-eval (Zhang et al., 2024a) for evaluation.

5.2 Datasets

In our paper, we mainly divided into 2 scenarios: Image Classification and MLLM Benchmark. The detailed information about datasets is described in Appendix B.1. For the image classification datasets, we choose 5 public classification datasets, including the small-scale dataset of CIFAR100 (Krizhevsky et al., 2009), the large-scale dataset of ImageNet-1K (Russakovsky et al., 2015), and the fine-grained datasets of CUB200 dataset (Wah et al., 2011), FGVC-Aircrafts dataset (Maji et al., 2013), and Stanford-Cars dataset (Krause et al., 2013). For the MLLM datasets, we choose 16 datasets, including visual question answering (VQAv2 (Goyal et al., 2017), GQA (Hudson & Manning, 2019), VizWiz (Gurari et al., 2018), ScienceVQA^{I} (Lu et al., 2022), TextVQA (Singh et al., 2019), MME-RealWorldQA (Zhang et al., 2025c)), understanding (MME (Perception) (Yin et al., 2023), MMBench (Liu et al., 2025), MMBench^{CN}, MMBench^{CC}, POPE (F1 score) (Li et al., 2023b), SEED^{I} (Li et al., 2023a), MM-Star (Chen et al., 2024b)), and reasoning (MMMU (Yue et al., 2024a), MMMU-Pro Standard (MMMU-Pro^{s}) (Yue et al., 2024b), MathVista (Lu et al., 2024)).

Table 3: The ImageNet-1K dataset classification results on Top1 Accuracy (Acc), Dynamic Forward, Throughput (TP/s) and FLOPs (G) in a NVIDIA A100. Forward$^{Dy.}$ denotes the metric through forward with dynamic.

Method	DeiT-Small			
	Forward$^{Dy.}$	TP/s	FLOPs (G)	Acc (%)
Vanilla	✗	1375.80	4.24	75.66
MixUp	✗	1374.54	4.24	77.80
CutMix	✗	1374.61	4.24	80.13
DeiT	✗	1374.20	4.24	79.80
TransMix	✗	1375.17	4.24	80.44
SMMix	✗	1373.93	4.24	79.36
MixPro	✗	1373.62	4.24	79.33
MergeMix	✓	**1591.66**	**3.56**	**80.71**

5.3 Implementations

In this subsection, we briefly introduce implementations on classification tasks and MLLM benchmarks (full details in Appendix B.2). For CIFAR100, ViT-based models (e.g., DeiT) use 224×224

Table 4: **Full system-level comparison results in LLaVA**. Compared with their counterparts. **AVG** denotes the average of the nine benchmarks for comprehensive comparison, except for MME, underline denotes MME with the sum of Perception and Cognition. Token^i denotes training with the token number. Full results in Table A10, Table A11 and Table A12.

Models	Token^i	Image Question Answering					Benchmarks					AVG	Gain
		VQAv2	GQA	VizWiz	SciVQA^I	TextVQA	MME	MMBench	MMBench^{CN}	POPE	SEED^I		
LLaVA Variants													
LLaVA-7B	Full	78.5	62.0	50.0	66.8	58.2	1510.7	64.3	58.3	85.87	66.19	65.57	–
LLaVA-NeXT-7B	Full	81.8	64.2	57.6	70.1	64.9	1519.0	67.4	60.6	86.5	70.2	69.3	–
LLaVA-NeXT-13B	Full	82.8	65.4	60.5	73.6	67.1	1575.0	70.0	64.4	86.2	71.9	71.3	–
SeVa-7B	Full	–	60.7	–	67.5	56.2	1450	65.6	59.2	86.7	65.8	–	–
SIMA	Full	–	62.2	54.4	68.1	58.3	1507.7	64.9	59.0	86.5	65.9	–	–
nSFT	Full	–	62.9	–	68.5	58.7	1531	67.1	61.0	86.8	66.2	–	–
LLaVA with Token Compressions													
LLaVA-PruMerge+	144	76.8	–	–	68.3	57.1	1462.4	64.9	–	84.0	–	–	–
VisionZip	192	77.4	60.1	–	68.2	57.8	1834.0	63.4	–	84.9	57.1	–	–
VisPrunner	128	75.8	58.2	52.7	69.1	57.0	1461.4	62.7	57.3	84.6	–	–	–
VScan	192	77.8	60.6	50.4	68.6	57.7	1806.0	63.9	57.4	86.2	–	–	–
LLaVA-Mini	1	77.6	60.9	56.2	70.4	57.0	1466.0	65.6	–	84.4	58.5	–	–
LLaVA with Augmentations & Ranking Loss													
SFT Vision	Full	**79.32**	**62.98**	47.45	70.05	57.17	**1490.88**	66.26	60.05	86.18	67.32	66.31	**+0.74**
+ MixUp	Full	79.27	62.58	44.95	69.41	57.39	1483.20	65.72	58.24	86.27	66.73	65.62	**+0.05**
+ CutMix	Full	79.18	62.40	45.04	**70.60**	57.06	1452.31	66.32	58.24	**86.47**	67.22	65.84	**+0.27**
+ ResizeMix	Full	77.78	61.66	44.43	68.91	55.11	1436.09	63.91	55.41	86.01	63.91	64.13	**-1.44**
+ MergeMix	Full	79.24	62.44	**47.69**	69.86	**57.56**	1479.97	**66.58**	**60.65**	86.10	**67.47**	**66.40**	**+0.83**
SFT Vision	288	78.6	**62.47**	48.15	69.51	56.41	**1486.24**	66.32	57.98	**87.37**	**66.75**	65.95	**+0.38**
+ MixUp	288	78.51	62.07	51.1	68.47	56.54	1459.06	65.63	**59.53**	86.86	66.06	66.08	**+0.51**
+ CutMix	288	78.58	62.39	50.53	**70.2**	55.95	1414.72	**66.92**	**59.53**	86.56	66.2	66.31	**+0.74**
+ ResizeMix	288	76.39	61.05	45.48	68.07	54.60	1447.35	63.31	51.97	86.57	62.54	63.33	**-2.24**
+ MergeMix	288	**78.61**	62.18	**52.14**	69.61	**56.85**	1453.97	66.58	59.02	86.47	66.63	**66.45**	**+0.88**

Table 5: **Full system-level comparison results in Qwen2.5-VL-Instruction (Qwen2.5-VL-Ins)**. **AVG** denotes the average of the nine benchmarks for comprehensive comparison.

Models	MMStar	MMBench	MMBench^{CN}	MMBench^{CC}	POPE	RWQA	MMMU	MMMU-Pro^s	MathVista	AVG	Gain
Qwen2.5-VL-Ins-7B	62.42	84.02	80.41	62.94	86.38	68.63	50.3	36.42	19.2	61.19	–
VisionThink-7B	61.00	82.73	81.01	**64.5**	87.65	69.28	**51.0**	37.27	23.8	62.03	**+0.84**
SFT Vision	62.66	83.41	81.01	63.52	**87.69**	68.63	50.89	36.7	**38.4**	63.66	**+1.47**
+ MergeMix	**62.92**	**84.19**	**81.18**	64.31	87.28	**70.46**	**51.0**	**37.46**	37.8	**64.07**	**+2.88**

images, trained with AdamW (weight decay 0.05), batch size 100, 200/600 epochs, RandomFlip/RandomCrop/RandAugment (Cubuk et al., 2020), and learning rates: 1e-3 (DeiT-Tiny/Small, cosine), 5e-4 (ViT-Small/Base), 2e-4 (ViT-Large). For ImageNet-1K, settings are consistent except 1e-3 learning rate, batch size 1024, 300 epochs (DeiT-Tiny/Small). For fine-grained datasets (CUB200, FGVC-Aircrafts, Stanford-Cars), DeiT-Small/ViT-Base are fine-tuned 200 epochs (batch size 16, 1e-5 lr) with PyTorch pretrained weights (Paszke et al., 2019).

Following LLaVA-v1.5, we use Vicuna-v1.5 7B (Chiang et al., 2023) (language decoder) and a 2-layer pre-trained MLP (visual-textual alignment, 1 epoch on `LCS-558K`), with a pre-trained CLIP vision encoder. SFT uses 1 epoch on `llava-v1.5-mix665k` (2e-5 lr, batch size 64, AdamW, 0.03 warmup, cosine scheduler), unfreezing the vision encoder (unlike LLaVA). For Qwen2.5-VL-Instruction, official checkpoints are fine-tuned 0.1 epoch on `llava-v1.5-mix665k` (similar settings); learning rates: 2e-6 (vision encoder), 1e-5 (LLM decoder/merger).

5.4 Results of Image Classification

We did the experiments on three classification datasets on a small-scale dataset (CIFAR100), a large-scale dataset (ImageNet-1K), and a fine-grained dataset (Stanford-Cars). **(1) CIFAR100:** Table 1 and Table A1 shows the part and full classification results respectively. MergeMix brings the **+2.15**%, **+2.51**% gains compared with TranMix on DeiT models. Gains **+2.87**%, **+2.88**% and

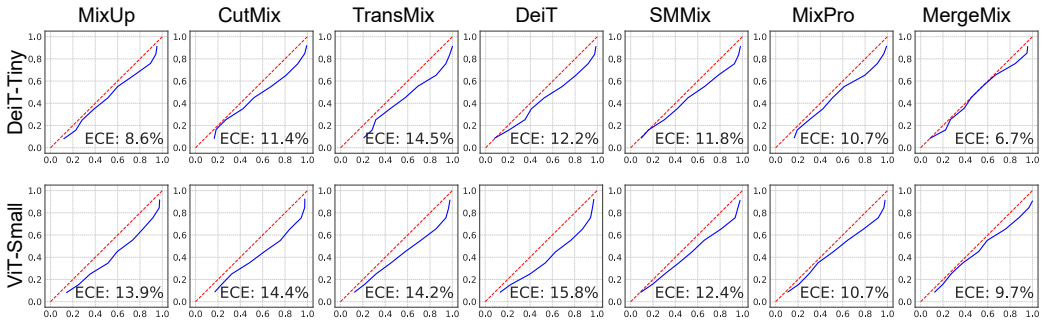

Figure 4: The confidence plots of mixup variants and MergeMix on the CIFAR100 dataset using DeiT-Tiny and ViT-Small. The red line indicates the expected prediction tendency.

Table 6: **The calibration results of LLaVA-v1.5-7B** on POPE, ScienceVQA^I, GQA & SEED^I. rl denotes training with ranking loss.

Method	GQA	POPE	SEED^I	ScienceVQA^I
Baseline	14.57	13.16	33.79	28.09
Training with Full Vision Tokens				
SFT Vision	8.52	12.82	32.67	21.66
+MixUp^{rl}	**6.09**	12.72	33.26	**21.51**
+CutMix^{rl}	6.74	**12.62**	32.77	24.71
+ResizeMix^{rl}	12.53	13.17	36.08	24.58
+MergeMix^{rl}	6.50	12.91	**32.52**	23.66
Training with 50% Vision Tokens				
SFT Vision	18.13	**12.67**	34.41	24.28
+MixUp^{rl}	13.40	12.74	33.60	22.61
+CutMix^{rl}	10.48	12.67	33.83	**20.63**
+ResizeMix^{rl}	12.60	12.97	37.41	23.74
+MergeMix^{rl}	**10.34**	12.76	**33.37**	25.22

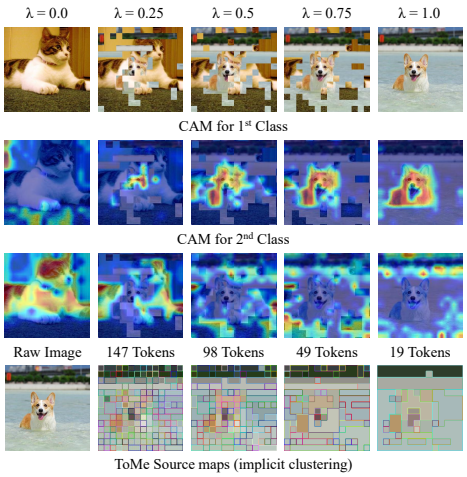

Figure 5: Visualization of MergeMix on different mixing ratios, including mixed images, Grad-CAM of top-2 logits, and ToMe source maps.

+4.79% on ViT models. All the results in Table 1 are trained for 200 epochs on the CIFAR100 dataset. **(2) Stanford-Cars:** Table 2 shows the fine-grain classification results on Stanford-Cars dataset. MergeMix achieves the **88.42**% and **92.20**% accuracy compared with other mixup methods. About the results of the CUB200 dataset and the FGVC-Aircrafts dataset in Table A2. **(3) ImageNet-1k:** Table 3 shows the results of accuracy, throughput, and flops on the ImageNet-1K dataset. It is notable that MergeMix brings a **+0.27**% gains and reduces **-0.68**G Flops compared with TransMix, and can also see other mixups with less throughput since they bring extra cost, but MergeMix has a high throughput of 1591.66 TP/s.

5.5 Results of MLLM Benchmarks

We chose two mainstream MLLMs for our experiments on the VQA tasks and reasoning. Table 4 shows the results of LLaVA benchmarks, with different vision tokens for training. With the setting of full vision tokens on the training stage, our method achieves an average gain of **+0.83%**. When reducing the vision token to 288, our method still performs well compared with SFT. A full comparison of results in Table A10, Table A11, and Table A12. In those different settings, MergeMix achieves an average performance of **66.84%**, improving over the LLaVA baseline by **+1.27%**. Table 5 shows the results of some VQA tasks and reasoning with Qwen2.5-VL-Instruction. MergeMix achieves an average gain of **+2.88%** over Qwen2.5-VL-Instruction. For the MathVista reasoning task, we reported the results without `LLM-as-the-judge-eval`. For the MMMU and MMMU-Pro tasks, we can achieve results on par with methods targeting reasoning improvements.

5.6 Results of Calibration

DNNs are prone to overconfidence in classification tasks. Mainfold Mixup (Verma et al., 2019) found that the mixup methods can effectively alleviate this problem. To this end, we compute the

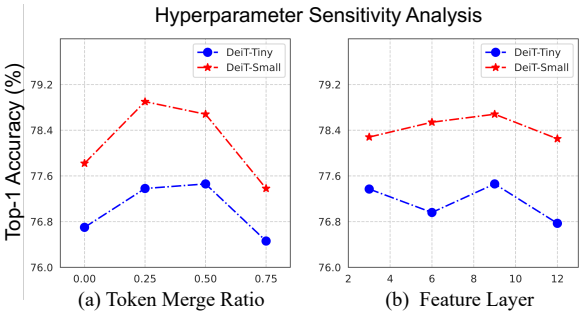

Figure 6: Sensitivity analysis study of 2 hyperparameters of MergMix. *Left:* Different merge ratios of backbones. *Right:* Attention score obtained from feature layer. Those results are from training for 200 epochs.

Table 7: Ablation study of MergeMix on classification trained 200 epochs.

Module	DeiT-Small	ViT-Small
Vanilla	65.81	62.64
+ TopK	75.80	75.19
+ ToMe	76.45	76.46
+ Re-Scaling λ	**78.68**	**77.02**

Table 8: Ablation study of MLLM training paradigm on LLaVA benchmark.

Method	VizWiz	SciVQA^{I}	MMBench
LLaVA-v1.5-7B	50.0	66.8	64.3
+ ToMe	50.45	68.86	62.8
+ SFT	48.15	69.51	66.32
+ MergeMix^{rl}	**52.14**	**69.61**	**66.58**

Expected Calibration Error (ECE (Guo et al., 2017)) of various mixup approaches on the CIFAR100 dataset for image classification. Also, to further analyze the calibration of MLLMs, we implement four short answer tasks, POPE, GQA, ScienceVQA, and SEED. Figure 4 shows the results of DeiT-Tiny and ViT-Small models trained for 200 epochs, showing that MergeMix obtains the best calibration of **6.7**% and **9.7**% in those ViT-specific mixup methods. (*i.e.*, TransMix, SMMix, and MixPro). Table 6 shows the results of the LLaVA baseline, LLaVA with SFT, and LLaVA with our approach. SFT reduces the ECE when tuning the vision encoder, with augmentation and ranking loss, which can be better since we bring in the reward signal for the model. The more comprehensive results of CIFAR100 and MLLM benchmark we plot in Table A3 and Table A9.

5.7 Ablation Study

The ablation study mainly focuses on three things. **(a)** Token merge module and optimized mixing ratio, whether efficient for image classification task; **(b)** Exploring the ability of vision encoder and the proposed training paradigm. For the image classification scenario, Table 7 shows that compared with TopK sampling, our token merge can improve performance with **+0.55%**, **+1.27%** gains respectively, which means token merge smooths the discrete attention score. The re-scaling mixing ratio further gains **+2.23%**, **+0.56%** on the CIFAR100 dataset. For the paradigm, we validate the token merge for the LLaVA-v1.5 7B model, further explore the training with an unfrozen vision encoder, and the ranking loss. Table 8 shows that, compared with vanilla Token Merge, unfreezing the vision encoder can perform better than freezing. The augmentation and ranking loss bring more performance than only the SFT loss; **(c)** For further exploring the performance of hyperparameters. We also evaluated the sensitivity of hyperparameters on MergeMix, *i.e.*, merged tokens and feature layer for better performance. Figure 6 shows the results of those hyperparameters.

6 Conclusion

This paper presents *MergeMix*, a unified augmentation for both image classification and MLLM alignment with token merge, also bridging the SFT and RL by building the preference pairs. Optimizing models through the mixed image and the raw image via a ranking loss. Extensive experiments demonstrate that MergeMix not only improves the performance on classic image classification tasks but also achieves a beneficial alignment and generalization on MLLM benchmarks. MergeMix provides a promising step toward a scalable, robust training paradigm for the multi-modal system.

Future Works There remain limitations in MergeMix for MLLMs. In future work, we will address them from two directions: **(1)** Data level: MergeMix currently enhances only the image modality, while text remains untouched. Extending mixup to the text modality could provide more fine-grained optimization. **(2)** Model level: The token-merging policy is static and unlearned. Making it learnable may further improve the mixing capability.

ACKNOWLEDGEMENT

This paper is supported by Young Scientists Fund of the National Natural Science Foundation of China (NSFC) (No. 62506305), Zhejiang Leading Innovative and Entrepreneur Team Introduction Program (No. 2024R01007), Key Research and Development Program of Zhejiang Province (No. 2025C01026), Scientific Research Project of Westlake University (No. WU2025WF003), Chinese Association for Artificial Intelligence (CAAI) & Ant Group Research Fund - AGI Track (No. 2025CAAI-ANT-13). It is also supported by the research funds of the National Talent Program and Hangzhou Municipal Talent Program.

REFERENCES

Kyungjune Baek, Duhyeon Bang, and Hyunjung Shim. Gridmix: Strong regularization through local context mapping. *Pattern Recognition*, 109, 2021. 3, 6

Shuai Bai, Keqin Chen, Xuejing Liu, Jialin Wang, Wenbin Ge, Sibo Song, Kai Dang, Peng Wang, Shijie Wang, Jun Tang, et al. Qwen2. 5-vl technical report. *arXiv preprint arXiv:2502.13923*, 2025. 1, 4, 7, 22

Daniel Bolya, Cheng-Yang Fu, Xiaoliang Dai, Peizhao Zhang, Christoph Feichtenhofer, and Judy Hoffman. Token merging: Your vit but faster. In *ICLR*, 2023. 3, 4

Jianjian Cao, Peng Ye, Shengze Li, Chong Yu, Yansong Tang, Jiwen Lu, and Tao Chen. Madtp: Multimodal alignment-guided dynamic token pruning for accelerating vision-language transformer. In *CVPR*, 2024. 3

Jie-Neng Chen, Shuyang Sun, Ju He, Philip HS Torr, Alan Yuille, and Song Bai. Transmix: Attend to mix for vision transformers. In *CVPR*, 2022. 3, 4, 6

Jieneng Chen, Luoxin Ye, Ju He, Zhao-Yang Wang, Daniel Khashabi, and Alan Yuille. Efficient large multi-modal models via visual context compression. In *NIPS*, 2024a. 3

Lin Chen, Jinsong Li, Xiaoyi Dong, Pan Zhang, Yuhang Zang, Zehui Chen, Haodong Duan, Jiaqi Wang, Yu Qiao, Dahua Lin, et al. Are we on the right way for evaluating large vision-language models? In *NIPS*, 2024b. 7, 17

Mengzhao Chen, Mingbao Lin, Zhihang Lin, Yuxin Zhang, Fei Chao, and Rongrong Ji. Smmix: Self-motivated image mixing for vision transformers. In *ICCV*, 2023. 3, 4, 6

Xueyi Chen, Keda Tao, Kele Shao, and Huan Wang. Streamingtom: Streaming token compression for efficient video understanding. *arXiv preprint arXiv:2510.18269*, 2025. 3

Wei-Lin Chiang, Zhuohan Li, Zi Lin, Ying Sheng, Zhanghao Wu, Hao Zhang, Lianmin Zheng, Siyuan Zhuang, Yonghao Zhuang, Joseph E Gonzalez, et al. Vicuna: An open-source chatbot impressing gpt-4 with 90%* chatgpt quality. *See https://vicuna. lmsys. org (accessed 14 April 2023)*, 2(3):6, 2023. 8, 18

Ekin D Cubuk, Barret Zoph, Jonathon Shlens, and Quoc V Le. Randaugment: Practical automated data augmentation with a reduced search space. In *CVPRW*, 2020. 8, 17

Ali Dabouei, Sobhan Soleymani, Fariborz Taherkhani, and Nasser M Nasrabadi. Supermix: Supervising the mixing data augmentation. In *CVPR*, 2021. 3

Sicheng Feng, Kaiwen Tuo, Song Wang, Lingdong Kong, Jianke Zhu, and Huan Wang. Rewardmap: Tackling sparse rewards in fine-grained visual reasoning via multi-stage reinforcement learning. *arXiv preprint arXiv:2510.02240*, 2025a. 19

Sicheng Feng, Song Wang, Shuyi Ouyang, Lingdong Kong, Zikai Song, Jianke Zhu, Huan Wang, and Xinchao Wang. Can mllms guide me home? a benchmark study on fine-grained visual reasoning from transit maps. *arXiv preprint arXiv:2505.18675*, 2025b. 19

Yash Goyal, Tejas Khot, Douglas Summers-Stay, Dhruv Batra, and Devi Parikh. Making the v in vqa matter: Elevating the role of image understanding in visual question answering. In *CVPR*, 2017. 7, 17

Chuan Guo, Geoff Pleiss, Yu Sun, and Kilian Q Weinberger. On calibration of modern neural networks. In *ICML*, 2017. 10

Dong Guo, Faming Wu, Feida Zhu, Fuxing Leng, Guang Shi, Haobin Chen, Haoqi Fan, Jian Wang, Jianyu Jiang, Jiawei Wang, et al. Seed1. 5-vl technical report. *arXiv preprint arXiv:2505.07062*, 2025. 22

Danna Gurari, Qing Li, Abigale J Stangl, Anhong Guo, Chi Lin, Kristen Grauman, Jiebo Luo, and Jeffrey P Bigham. Vizwiz grand challenge: Answering visual questions from blind people. In *CVPR*, 2018. 7, 17

Ethan Harris, Antonia Marcu, Matthew Painter, Mahesan Niranjan, and Adam Prügel-Bennett Jonathon Hare. Fmix: Enhancing mixed sample data augmentation. *arXiv preprint arXiv:2002.12047*, 2020. 3, 6

Yefei He, Feng Chen, Jing Liu, Wenqi Shao, Hong Zhou, Kaipeng Zhang, and Bohan Zhuang. Zipvl: Efficient large vision-language models with dynamic token sparsification. *arXiv preprint arXiv:2410.08584*, 2024. 3

Wei-Ning Hsu, Benjamin Bolte, Yao-Hung Hubert Tsai, Kushal Lakhotia, Ruslan Salakhutdinov, and Abdelrahman Mohamed. Hubert: Self-supervised speech representation learning by masked prediction of hidden units. *IEEE/ACM transactions on audio, speech, and language processing*, pp. 3451–3460, 2021. 21

Drew A Hudson and Christopher D Manning. Gqa: A new dataset for real-world visual reasoning and compositional question answering. In *CVPR*, 2019. 7, 17

Khawar Islam, Muhammad Zaigham Zaheer, Arif Mahmood, and Karthik Nandakumar. Diffusemix: Label-preserving data augmentation with diffusion models. In *CVPR*, 2024a. 3

Khawar Islam, Muhammad Zaigham Zaheer, Arif Mahmood, Karthik Nandakumar, and Naveed Akhtar. Genmix: effective data augmentation with generative diffusion model image editing. *arXiv preprint arXiv:2412.02366*, 2024b. 3

Xin Jin, Hongyu Zhu, Siyuan Li, Zedong Wang, Zicheng Liu, Juanxi Tian, Chang Yu, Huafeng Qin, and Stan Z Li. A survey on mixup augmentations and beyond. *arXiv preprint arXiv:2409.05202*, 2024a. 5

Xin Jin, Hongyu Zhu, Mounîm A El Yacoubi, Haiyang Li, Hongchao Liao, Huafeng Qin, and Yun Jiang. Starlknet: Star mixup with large kernel networks for palm vein identification. *arXiv preprint arXiv:2405.12721*, 2024b. 3

Minsoo Kang and Suhyun Kim. Guidedmixup: an efficient mixup strategy guided by saliency maps. In *AAAI*, 2023. 6

Jang-Hyun Kim, Wonho Choo, and Hyun Oh Song. Puzzle mix: Exploiting saliency and local statistics for optimal mixup. In *ICML*, 2020. 3, 6

Jang-Hyun Kim, Wonho Choo, Hosan Jeong, and Hyun Oh Song. Co-mixup: Saliency guided joint mixup with supermodular diversity. *arXiv preprint arXiv:2102.03065*, 2021. 3

Jonathan Krause, Michael Stark, Jia Deng, and Li Fei-Fei. 3d object representations for fine-grained categorization. In *3DRR-13)*, 2013. 7, 17

Alex Krizhevsky, Geoffrey Hinton, et al. Learning multiple layers of features from tiny images. 2009. 7, 17

Zhibin Lan, Liqiang Niu, Fandong Meng, Wenbo Li, Jie Zhou, and Jinsong Su. Avg-llava: An efficient large multimodal model with adaptive visual granularity. In *ACL*, 2025. 3

Jin-Ha Lee, Muhammad Zaigham Zaheer, Marcella Astrid, and Seung-Ik Lee. Smoothmix: a simple yet effective data augmentation to train robust classifiers. In *CVPRW*, 2020. 3, 6

Bohao Li, Rui Wang, Guangzhi Wang, Yuying Ge, Yixiao Ge, and Ying Shan. Seed-bench: Benchmarking multimodal llms with generative comprehension. *arXiv preprint arXiv:2307.16125*, 2023a. 7, 17

Siyuan Li, Zedong Wang, Zicheng Liu, Di Wu, and Stan Z. Li. Openmixup: Open mixup toolbox and benchmark for visual representation learning. *arXiv preprint arXiv:2209.04851*, 2022. 6, 18

Wentong Li, Yuqian Yuan, Jian Liu, Dongqi Tang, Song Wang, Jie Qin, Jianke Zhu, and Lei Zhang. Tokenpacker: Efficient visual projector for multimodal llm. *IJCV*, pp. 1–19, 2025. 3

Yifan Li, Yifan Du, Kun Zhou, Jinpeng Wang, Xin Zhao, and Ji-Rong Wen. Evaluating object hallucination in large vision-language models. In *NIPS*, 2023b. 7, 17

Haotian Liu, Chunyuan Li, Yuheng Li, Bo Li, Yuanhan Zhang, Sheng Shen, and Yong Jae Lee. Llava-next: Improved reasoning, ocr, and world knowledge, 2024a. URL https://llava-vl.github.io/blog/2024-01-30-llava-next/. 7

Haotian Liu, Chunyuan Li, Qingyang Wu, and Yong Jae Lee. Visual instruction tuning. In *NIPS*, 2024b. 1, 4, 6

Ting Liu, Liangtao Shi, Richang Hong, Yue Hu, Quanjun Yin, and Linfeng Zhang. Multi-stage vision token dropping: Towards efficient multimodal large language model. *arXiv preprint arXiv:2411.10803*, 2024c. 3

Yuan Liu, Haodong Duan, Yuanhan Zhang, Bo Li, Songyang Zhang, Wangbo Zhao, Yike Yuan, Jiaqi Wang, Conghui He, Ziwei Liu, et al. Mmbench: Is your multi-modal model an all-around player? In *ECCV*, 2025. 7, 17

Zicheng Liu, Siyuan Li, Di Wu, Zihan Liu, Zhiyuan Chen, Lirong Wu, and Stan Z Li. Automix: Unveiling the power of mixup for stronger classifiers. In *ECCV*, 2022. 3, 6

Zicheng Liu, Siyuan Li, Ge Wang, Lirong Wu, Cheng Tan, and Stan Z Li. Harnessing hard mixed samples with decoupled regularizer. In *NIPS*, 2023. 5

Pan Lu, Swaroop Mishra, Tanglin Xia, Liang Qiu, Kai-Wei Chang, Song-Chun Zhu, Oyvind Tafjord, Peter Clark, and Ashwin Kalyan. Learn to explain: Multimodal reasoning via thought chains for science question answering. In *NIPS*, 2022. 7, 17

Pan Lu, Hritik Bansal, Tony Xia, Jiacheng Liu, Chunyuan Li, Hannaneh Hajishirzi, Hao Cheng, Kai-Wei Chang, Michel Galley, and Jianfeng Gao. Mathvista: Evaluating mathematical reasoning of foundation models in visual contexts. In *ICLR*, 2024. 7, 17

Tiange Luo, Ang Cao, Gunhee Lee, Justin Johnson, and Honglak Lee. Probing visual language priors in vlms. *arXiv preprint arXiv:2501.00569*, 2024. 1

Subhransu Maji, Esa Rahtu, Juho Kannala, Matthew Blaschko, and Andrea Vedaldi. Fine-grained visual classification of aircraft. *arXiv preprint arXiv:1306.5151*, 2013. 7, 17

Yu Meng, Mengzhou Xia, and Danqi Chen. Simpo: Simple preference optimization with a reference-free reward. In *NIPS*, 2024. 6

Adam Paszke, Sam Gross, Francisco Massa, Adam Lerer, James Bradbury, Gregory Chanan, Trevor Killeen, Zeming Lin, Natalia Gimelshein, Luca Antiga, Alban Desmaison, Andreas Köpf, Edward Yang, Zach DeVito, Martin Raison, Alykhan Tejani, Sasank Chilamkurthy, Benoit Steiner, Lu Fang, Junjie Bai, and Soumith Chintala. Pytorch: An imperative style, high-performance deep learning library. In *Advances in Neural Information Processing Systems (NeurIPS)*, 2019. 8, 18

Karol J Piczak. Esc: Dataset for environmental sound classification. In *ACMMM*, 2015. 21

Huafeng Qin, Xin Jin, Yun Jiang, Mounim A El-Yacoubi, and Xinbo Gao. Adversarial automixup. In *ICLR*, 2024a. 3, 6

Huafeng Qin, Xin Jin, Hongyu Zhu, Hongchao Liao, Mounîm A El-Yacoubi, and Xinbo Gao. Sumix: Mixup with semantic and uncertain information. In *ECCV*, 2024b. 5

Jie Qin, Jiemin Fang, Qian Zhang, Wenyu Liu, Xingang Wang, and Xinggang Wang. Resizemix: Mixing data with preserved object information and true labels. *arXiv preprint arXiv:2012.11101*, 2020. 3, 6

Alec Radford, Jong Wook Kim, Chris Hallacy, Aditya Ramesh, Gabriel Goh, Sandhini Agarwal, Girish Sastry, Amanda Askell, Pamela Mishkin, Jack Clark, et al. Learning transferable visual models from natural language supervision. In *ICML*, 2021. 17

Rafael Rafailov, Archit Sharma, Eric Mitchell, Christopher D Manning, Stefano Ermon, and Chelsea Finn. Direct preference optimization: Your language model is secretly a reward model. In *NIPS*, 2023. 1, 4

Olga Russakovsky, Jia Deng, Hao Su, Jonathan Krause, Sanjeev Satheesh, Sean Ma, Zhiheng Huang, Andrej Karpathy, Aditya Khosla, Michael Bernstein, Alexander C. Berg, and Li Fei-Fei. ImageNet Large Scale Visual Recognition Challenge. *IJCV*, 115(3):211–252, 2015. 7, 17

Justin Salamon, Christopher Jacoby, and Juan Pablo Bello. A dataset and taxonomy for urban sound research. In *ACMMM*, 2014. 21

John Schulman, Filip Wolski, Prafulla Dhariwal, Alec Radford, and Oleg Klimov. Proximal policy optimization algorithms. *arXiv preprint arXiv:1707.06347*, 2017. 4

Ramprasaath R. Selvaraju, Michael Cogswell, Abhishek Das, Ramakrishna Vedantam, Devi Parikh, and Dhruv Batra. Grad-cam: Visual explanations from deep networks via gradient-based localization. *arXiv preprint arXiv:1610.02391*, 2019. 26, 29

Yuzhang Shang, Mu Cai, Bingxin Xu, Yong Jae Lee, and Yan Yan. Llava-prumerge: Adaptive token reduction for efficient large multimodal models. *arXiv preprint arXiv:2403.15388*, 2024. 3, 7

Kele Shao, Keda Tao, Can Qin, Haoxuan You, Yang Sui, and Huan Wang. Holitom: Holistic token merging for fast video large language models. *arXiv preprint arXiv:2505.21334*, 2025. 3

Amanpreet Singh, Vivek Natarajan, Meet Shah, Yu Jiang, Xinlei Chen, Dhruv Batra, Devi Parikh, and Marcus Rohrbach. Towards vqa models that can read. In *CVPR*, 2019. 7, 17

Shuyang Sun, Jie-Neng Chen, Ruifei He, Alan Yuille, Philip Torr, and Song Bai. Lumix: Improving mixup by better modelling label uncertainty. *arXiv preprint arXiv:2211.15846*, 2022. 5

Wentao Tan, Qiong Cao, Yibing Zhan, Chao Xue, and Changxing Ding. Beyond human data: Aligning multimodal large language models by iterative self-evolution. In *AAAI*, 2025. 1

Keda Tao, Can Qin, Haoxuan You, Yang Sui, and Huan Wang. Dycoke: Dynamic compression of tokens for fast video large language models. In *CVPR*, 2025a. 3

Keda Tao, Kele Shao, Bohan Yu, Weiqiang Wang, Huan Wang, et al. Omnizip: Audio-guided dynamic token compression for fast omnimodal large language models. *arXiv preprint arXiv:2511.14582*, 2025b. 3

Gemini Team, Rohan Anil, Sebastian Borgeaud, Jean-Baptiste Alayrac, Jiahui Yu, Radu Soricut, Johan Schalkwyk, Andrew M Dai, Anja Hauth, Katie Millican, et al. Gemini: a family of highly capable multimodal models. *arXiv preprint arXiv:2312.11805*, 2023. 22

Peter Tong, Ellis Brown, Penghao Wu, Sanghyun Woo, Adithya Jairam Vedagiri IYER, Sai Charitha Akula, Shusheng Yang, Jihan Yang, Manoj Middepogu, Ziteng Wang, et al. Cambrian-1: A fully open, vision-centric exploration of multimodal llms. In *NIPS*, 2024. 1

Hugo Touvron, Matthieu Cord, Matthijs Douze, Francisco Massa, Alexandre Sablayrolles, and Herve Jegou. Training data-efficient image transformers & distillation through attention. In *ICML*, 2021. 6

AFM Shahab Uddin, Mst Sirazam Monira, Wheemyung Shin, TaeChoong Chung, and Sung-Ho Bae. Saliencymix: A saliency guided data augmentation strategy for better regularization. In *ICLR*, 2021. 3, 6

Pavan Kumar Anasosalu Vasu, Fartash Faghri, Chun-Liang Li, Cem Koc, Nate True, Albert Antony, Gokula Santhanam, James Gabriel, Peter Grasch, Oncel Tuzel, et al. Fastvlm: Efficient vision encoding for vision language models. In *CVPR*, 2025. 3

Vikas Verma, Alex Lamb, Christopher Beckham, Amir Najafi, Ioannis Mitliagkas, David Lopez-Paz, and Yoshua Bengio. Manifold mixup: Better representations by interpolating hidden states. In *ICML*, 2019. 9

Catherine Wah, Steve Branson, Peter Welinder, Pietro Perona, and Serge Belongie. The caltech-ucsd birds-200-2011 dataset. California Institute of Technology, 2011. 7, 17

Devesh Walawalkar, Zhiqiang Shen, Zechun Liu, and Marios Savvides. Attentive cutmix: An enhanced data augmentation approach for deep learning based image classification. In *ICASSP*, 2020. 3, 6

Chenru Wang, Beier Zhu, and Chi Zhang. Free lunch for stabilizing rectified flow inversion. *arXiv preprint arXiv:2602.11850*, 2026. 19

Fei Wang, Wenxuan Zhou, James Y Huang, Nan Xu, Sheng Zhang, Hoifung Poon, and Muhao Chen. mdpo: Conditional preference optimization for multimodal large language models. In *EMNLP*, 2024a. 25

Xiyao Wang, Jiuhai Chen, Zhaoyang Wang, Yuhang Zhou, Yiyang Zhou, Huaxiu Yao, Tianyi Zhou, Tom Goldstein, Parminder Bhatia, Furong Huang, et al. Enhancing visual-language modality alignment in large vision language models via self-improvement. *arXiv preprint arXiv:2405.15973*, 2024b. 1, 7

Zhiming Wang, Lin Gu, and Feng Lu. Tdattenmix: Top-down attention guided mixup. In *AAAI*, 2025. 6

Long Xing, Qidong Huang, Xiaoyi Dong, Jiajie Lu, Pan Zhang, Yuhang Zang, Yuhang Cao, Conghui He, Jiaqi Wang, Feng Wu, et al. Pyramiddrop: Accelerating your large vision-language models via pyramid visual redundancy reduction. *arXiv preprint arXiv:2410.17247*, 2024. 3

Shuo Xing, Peiran Li, Yuping Wang, Ruizheng Bai, Yueqi Wang, Chan-Wei Hu, Chengxuan Qian, Huaxiu Yao, and Zhengzhong Tu. Re-align: Aligning vision language models via retrieval-augmented direct preference optimization. In *EMNLP*, 2025. 25

An Yang, Anfeng Li, Baosong Yang, Beichen Zhang, Binyuan Hui, Bo Zheng, Bowen Yu, Chang Gao, Chengen Huang, Chenxu Lv, et al. Qwen3 technical report. *arXiv preprint arXiv:2505.09388*, 2025a. 22

Senqiao Yang, Yukang Chen, Zhuotao Tian, Chengyao Wang, Jingyao Li, Bei Yu, and Jiaya Jia. Visionzip: Longer is better but not necessary in vision language models. In *CVPR*, 2025b. 3, 7

Senqiao Yang, Junyi Li, Xin Lai, Bei Yu, Hengshuang Zhao, and Jiaya Jia. Visionthink: Smart and efficient vision language model via reinforcement learning. *arXiv preprint arXiv:2507.13348*, 2025c. 1, 7

Xubing Ye, Yukang Gan, Yixiao Ge, Xiao-Ping Zhang, and Yansong Tang. Atp-llava: Adaptive token pruning for large vision language models. In *CVPR*, 2025. 3

Shukang Yin, Chaoyou Fu, Sirui Zhao, Ke Li, Xing Sun, Tong Xu, and Enhong Chen. A survey on multimodal large language models. *arXiv preprint arXiv:2306.13549*, 2023. 7, 17

Weihao Yu, Mi Luo, Pan Zhou, Chenyang Si, Yichen Zhou, Xinchao Wang, Jiashi Feng, and Shuicheng Yan. Metaformer is actually what you need for vision. In *CVPR*, 2022. 21

Xiang Yue, Yuansheng Ni, Kai Zhang, Tianyu Zheng, Ruoqi Liu, Ge Zhang, Samuel Stevens, Dongfu Jiang, Weiming Ren, Yuxuan Sun, et al. Mmmu: A massive multi-discipline multimodal understanding and reasoning benchmark for expert agi. In *CVPR*, 2024a. 7, 17

Xiang Yue, Tianyu Zheng, Yuansheng Ni, Yubo Wang, Kai Zhang, Shengbang Tong, Yuxuan Sun, Botao Yu, Ge Zhang, Huan Sun, et al. Mmmu-pro: A more robust multi-discipline multimodal understanding benchmark. *arXiv preprint arXiv:2409.02813*, 2024b. 7, 17

Sangdoo Yun, Dongyoon Han, Seong Joon Oh, Sanghyuk Chun, Junsuk Choe, and Youngjoon Yoo. Cutmix: Regularization strategy to train strong classifiers with localizable features. In *ICCV*, 2019. 3, 6

Ce Zhang, Kaixin Ma, Tianqing Fang, Wenhao Yu, Hongming Zhang, Zhisong Zhang, Yaqi Xie, Katia Sycara, Haitao Mi, and Dong Yu. Vscan: Rethinking visual token reduction for efficient large vision-language models. *arXiv preprint arXiv:2505.22654*, 2025a. 7

Hongyi Zhang, Moustapha Cisse, Yann N Dauphin, and David Lopez-Paz. mixup: Beyond empirical risk minimization. *arXiv preprint arXiv:1710.09412*, 2017. 3, 6

Kaichen Zhang, Bo Li, Peiyuan Zhang, Fanyi Pu, Joshua Adrian Cahyono, Kairui Hu, Shuai Liu, Yuanhan Zhang, Jingkang Yang, Chunyuan Li, and Ziwei Liu. Lmms-eval: Reality check on the evaluation of large multimodal models. *arXiv preprint arXiv:407.12772*, 2024a. 7, 17

Qizhe Zhang, Aosong Cheng, Ming Lu, Renrui Zhang, Zhiyong Zhuo, Jiajun Cao, Shaobo Guo, Qi She, and Shanghang Zhang. Beyond text-visual attention: Exploiting visual cues for effective token pruning in vlms. *arXiv preprint arXiv:2412.01818*, 2024b. 7

Shaolei Zhang, Qingkai Fang, Zhe Yang, and Yang Feng. Llava-mini: Efficient image and video large multimodal models with one vision token. In *ICLR*, 2025b. 7

YiFan Zhang, Huanyu Zhang, Haochen Tian, Chaoyou Fu, Shuangqing Zhang, Junfei Wu, Feng Li, Kun Wang, Qingsong Wen, Zhang Zhang, et al. Mme-realworld: Could your multimodal llm challenge high-resolution real-world scenarios that are difficult for humans? In *ICLR*, 2025c. 7, 17

Qihao Zhao, Yangyu Huang, Wei Hu, Fan Zhang, and Jun Liu. Mixpro: Data augmentation with maskmix and progressive attention labeling for vision transformer. In *ICLR*, 2023. 3, 4, 6

Junhan Zhu, Hesong Wang, Mingluo Su, Zefang Wang, and Huan Wang. Obs-diff: Accurate pruning for diffusion models in one-shot. *arXiv preprint arXiv:2510.06751*, 2025a. 3

Ke Zhu, Liang Zhao, Zheng Ge, and Xiangyu Zhang. Self-supervised visual preference alignment. In *ACMMM*, 2024. 1, 7

Ke Zhu, Yu Wang, Yanpeng Sun, Qiang Chen, Jiangjiang Liu, Gang Zhang, and Jingdong Wang. Continual sft matches multimodal rlhf with negative supervision. In *CVPR*, 2025b. 1, 7

A Declaration of LLM Usage

We use the Large Language Models (LLMs) for this paper to serve one purpose: to aid and polish the paper writing. We use the LLMs in a very limited capacity, restricted to minor editing of grammar, phrasing, and readability. We do not involve the LLMs in designing the method, developing theoretical results, and conducting experiments.

B Detail Information

B.1 Datasets

Image Classification. We choose five mainstream classification datasets: **(i)** CIFAR100 dataset (Krizhevsky et al., 2009) consists of 100 classes of color images with a resolution of 32 $\times$ 32 pixels, containing 50,000 training images and 10,000 test images. **(ii)** ImageNet-1k dataset (Russakovsky et al., 2015) consists of 1,000 classes with varied image resolutions commonly cropped to 224 $\times$ 224 pixels, containing 1,281,167 training images and 50,000 test images. **(iii)** CUB200 dataset (Wah et al., 2011) contains 200 bird species, including total 11,788 images, we divided 5,994 images as training images and 5,794 images as test images, **(iv)** FGVC-Aircrafts dataset (Maji et al., 2013) contains 100 aircraft model classes, including 6,667 training images and 3,333 test images, **(v)** Stanford-Cars dataset (Krause et al., 2013) contains 196 car model classes, including 8,144 training images and 8,041 test images. All the fine-grained datasets we used set the resolution as 224 $\times$ 224 pixels for training and testing.

MLLM Benchmark. we conducted various experiments on LLaVA Benchmark and lmms-eval (Zhang et al., 2024a), which based on 16 datasets: **(i)** VQAv2 dataset (Goyal et al., 2017) contains 204,721 training images, 22,000 validation images, and 40,504 test images, **(ii)** GQA dataset (Hudson & Manning, 2019) focuses on graph-based reasoning with 220,000 training images and 150,000 validation/test questions, **(iii)** VizWiz dataset (Gurari et al., 2018) images are captured by mobile devices with questions from visually impaired users (31,173 training images), **(iv)** ScienceVQA dataset (Lu et al., 2022), **(v)** TextVQA dataset (Singh et al., 2019), and **(vi)** SEED dataset (Li et al., 2023a) contain 21,208, 28,408, and 15,000 training images, respectively, emphasizing scientific reasoning, text understanding, and multi-modal reasoning. **(vii)** MME dataset (Yin et al., 2023) and **(viii)** MMBench dataset (Liu et al., 2025) provide general multi-modal evaluation, **(ix)** $\text{MMBench}^{\text{CN}}$ dataset as the Chinese version of MMbench, **(x)** $\text{MMBench}^{\text{CC}}$ dataset as the Cross Check version of MMbench. **(xi)** POPE dataset (Li et al., 2023b) evaluates performance on prompt-driven tasks with zero-shot and few-shot settings. **(xii) & (xiii)** MMMU & MMMU-Pro datasets (Yue et al., 2024a;b) are a multi-modal reasoning benchmark with college-level exam questions, **(xiv)** MME-RealWorldQA dataset (Zhang et al., 2025c) emphasizes real-world, long-tail visual understanding in everyday scenarios. **(xv)** MMStar dataset (Chen et al., 2024b) uses testing star-level multi-modal reasoning across diverse tasks. **(xvi)** MathVista dataset (Lu et al., 2024) for the visual mathematical reasoning by involving geometry, algebra, and charts. For the LLaVA benchmark, all images are typically cropped or resized to 336 $\times$ 336 pixels for training and evaluation since the CLIP (Radford et al., 2021) is the vision encoder. For the Qwen2.5-VL-Instruction benchmark, the images are dynamically scaled by the Qwen-VL model.

B.2 Implementations

Classification tasks: **(i)** For the CIFAR100 dataset, aiming to be suitable for training ViT-based approaches, *e.g.*, DeiT, we resize images to 224 $\times$ 224 and train them with the AdamW optimizer with weight decay of 0.05, batch size of 100, and total training of 200 epochs and 600 epochs. Uses RandomFlip and RandomCrop as basic augmentations, and additionally, we use RandAugment (Cubuk et al., 2020). For DeiT-Tiny and DeiT-Small, we use the learning rate of 1e-3 with a dynamic cosine scheduler. For ViT-Small and ViT-Base models, we set the learning rate to 5e-4, the learning rate of ViT-Large up to 2e-4, all dynamically adjusted by a cosine scheduler. **(ii)** For the ImageNet-1K dataset, the dataset settings are the same as CIFAR100, but we use the learning rate as 1e-3, batch size of 1024, and a total training of 300 epochs for DeiT-Tiny and DeiT-Small with AdamW optimizer with weight decay of 0.05. **(iii)** For all fine-grain datasets, *i.e.*, CUB-200 dataset, FGVC-Aircrafts dataset, and Stanford-Cars dataset, we fine-tune the DeiT-Small and ViT-

Table A1: Top-1 accuracy (%) of mixup methods on CIFAR-100 dataset under DeiT-Tiny/Small, ViT-Small/Base/Large different model sizes. The α parameter of the Beta distribution follows the setting in OpenMixup (Li et al., 2022) setting.

Method	DeiT-Tiny		DeiT-Small		ViT-Small		ViT-Base		ViT-Large
	200 epochs	600 epochs	200 epochs	600 epochs	200 epochs	600 epochs	200 epochs	600 epochs	200 epochs
Vanilla	64.70	66.70	65.81	68.50	62.64	66.32	63.33	66.47	61.83
MixUp	69.47	73.06	69.98	76.35	68.67	73.57	69.66	73.90	67.90
CutMix	75.98	79.60	74.21	79.54	69.67	76.66	72.18	71.94	68.97
FMix	72.73	77.24	70.41	74.31	68.41	72.55	68.62	71.10	66.12
GridMix	71.54	76.23	68.86	74.96	70.15	68.23	66.63	68.49	63.20
ResizeMix	69.42	72.98	68.54	71.95	67.86	69.09	63.72	69.33	63.48
SaliencyMix	69.83	75.45	69.78	76.60	70.14	74.09	68.75	75.50	67.12
PuzzleMix	73.40	79.96	73.60	**81.01**	70.92	78.44	71.13	**79.49**	69.77
AutoMix	72.91	**81.16**	**76.24**	**80.91**	68.44	77.73	**73.40**	–	72.10
AdAutoMix	72.83	77.97	72.63	78.94	69.66	–	71.43	–	69.69
DeiT	74.01	79.90	75.92	79.54	72.96	77.60	72.15	76.26	69.23
TransMix	75.31	80.66	76.17	79.33	74.15	78.27	72.87	77.89	71.40
SMMix	73.84	78.62	74.09	79.84	73.50	79.65	70.87	78.18	71.38
MixPro	74.78	80.19	75.26	79.55	73.49	**80.02**	73.18	78.69	**72.28**
MergeMix	**77.46**	**81.20**	**78.68**	80.39	**77.02**	**81.44**	**75.75**	**79.59**	**76.19**

Table A2: Top-1 accuracy (%) of mixup methods on Fine-Grained datasets: CUB200, FGVC-Aircrafts, and Stanford-Cars.

Method	α	CUB200		FGVC-Aircrafts		Stanford-Cars	
		DeiT-Small	ViT-Base	DeiT-Small	ViT-Base	DeiT-Small	ViT-Base
Vanilla	–	82.05	88.00	77.59	80.86	86.77	91.31
MixUp	1.0	84.31	**88.75**	**78.52**	**82.18**	87.73	91.36
CutMix	0.2	81.69	87.76	75.67	80.08	88.37	91.53
SmoothMix	0.2	83.87	87.02	75.31	76.72	86.39	90.88
FMix	0.2	82.64	**88.68**	77.08	79.33	87.18	91.36
GridMix	0.2	82.34	87.23	75.85	78.49	87.58	91.31
ResizeMix	1.0	82.15	87.61	74.59	77.62	87.45	91.59
Attentive-CutMix	2.0	82.83	87.47	75.04	76.06	87.35	90.29
SaliencyMix	0.2	82.34	87.92	77.98	79.81	87.94	91.47
PuzzleMix	1.0	84.39	88.23	78.28	81.27	88.60	91.83
GuidedMix^{ap}	1.0	**84.71**	88.26	77.05	79.24	86.99	90.40
DeiT	0.2	84.04	88.47	75.89	81.07	88.72	**92.17**
TransMix	1.0	83.34	88.10	75.73	77.77	88.38	91.66
SMMix	1.0	82.88	88.35	76.42	78.40	**88.76**	91.93
MixPro	1.0	82.31	86.93	75.25	75.97	88.38	91.48
MergeMix	1.0	**85.40**	88.40	**80.92**	**81.97**	**89.42**	**92.20**

Base model for 200 epochs with a batch size of 16, learning rate of 1e-5, loading the pre-trained model weight from PyTorch (Paszke et al., 2019).

MLLM benchmark: Following the LLaVA-v1.5 settings, we use a pre-trained Vicuna-v1.5 7B (Chiang et al., 2023) as the language decoder, which uses a pre-trained 2 $\times$ MLP as the projection for aligning the vision and text modistes, which was trained for one epoch on `LCS-558K`. For the vision encoder, we use a pre-trained CLIP encoder and extract the visual representation from the input images. For SFT, the learning rate was set as 2e-5, the batch size was 64, and training one epoch on `llava-v1.5-mix665k` dataset, uses AdamW optimizer with (0.9, 0.999) betas and epsilon of 1e-8, warmup ratio of 0.03 with a cosine scheduler. The difference from LLaVA is that we unfreeze the vision encoder during training. About Qwen2.5-VL-Instruction, we fine-tune with `llava-v1.5-mix665k` dataset for 0.1 epoch, uses AdamW optimizer with (0.9, 0.999) betas and epsilon of 1e-8 like LLaVA, warmup with 0.03 ratio. The learning rate of the vision encoder, LLM decoder, and merger were set to 2e-6, 1e-5, and 1e-5, respectively.

Algorithm 1 MergeMix for Image Classification

```
# Inputs: vision model f_θ(·), training parameters θ of model, dataset D, mixup parameter α; output: updated f_θ(·)
#  sample a paired mini-batch from D (two images and labels)
1: for (x_i, y_i), (x_j, y_j) in DataLoader(D):
#  sample mixup ratio λ (shared with Alg. 2)
2:   λ ~ Beta(α, α)
3:   M, λ̂ = P(x_i, x_j, λ)
#  lines 3--4: MergeMix augmentation (same core as Alg. 2)
4:   x̂ = M ⊙ x_i + (1 − M) ⊙ x_j
5:   logits = f_θ(x̂)
#  main supervised loss on mixed sample (parallels L_SFT in Alg. 2)
6:   L_MCE = λ̂ · L_CE(logits, y_i) + (1 − λ̂) · L_CE(logits, y_j)
#  optional regularizer for augmentation consistency
7:   L_CE = f_θ(x, y)
8:   L_Total = L_MCE + L_CE
9:   L_Total.backward()
10:  optimizer.step()
11:  optimizer.zero_grad()
```

Algorithm 2 MergeMix for MLLM Alignment

```
# Inputs: MLLM π_θ(·), learnable parameters θ of model, dataset D of (x, q, T); output: updated π_θ(·)
#  iterate over triples
1: for (x, q, T) in DataLoader(D):
#  sample an auxiliary image x_i (mirrors mix partner in Alg. 1)
2:   (x_i, _) = randomSample(D)
3:   M = P(x, x_i)
#  lines 3--4: same MergeMix augmentation core as Alg. 1
4:   x̂ = M ⊙ x + (1 − M) ⊙ x_i
#  winner (raw) vs. loser (mixed) outputs for the same prompt
5:   Y_w = π_θ(x, q)
6:   Y_l = π_θ(x̂, q)
#  supervised fine-tuning loss (analogous to L_CE in Alg. 1)
7:   L_SFT = L_CE(Y_w, T)
8:   s_w = AvgLogProb(Y_w, T)
9:   s_l = AvgLogProb(Y_l, T)
#  preference loss (SimPO) that prefers winner over loser
10:  L^Mix_SimPO = −log σ(s_w − s_l − λ)
11:  L_Total = L_SFT + L^Mix_SimPO
12:  L_Total.backward()
13:  optimizer.step()
14:  optimizer.zero_grad()
```

B.3 Algorithms

Algorithm 1 and Algorithm 2 show the pseudo codes for MergeMix on both image classification and preference tuning.

B.4 Future work

There are still some shortcomings in MergeMix for MLLMs. In future work, we will explore this from: **(1)** From the data perspective: MergeMix focuses on the enhancement of the image modality during training, while text inputs still remain raw. How to extend mixup to the text modality in MLLM tasks needs to be solved, as this can provide more fine-grained optimization guidelines. **(2)** From the model perspective: The token merging is still static and unlearned. Improving the merging strategy to make it learnable via metrics or backpropagation could enhance the token merging ability for mixing. **(3)** How to use sampling to find the optimal candidate as the loser from multiple augmented data, like RL-based methods (Feng et al., 2025b;a) and how to construct high-quality losers when adopting image editing methods (Wang et al., 2026) are also promising ways to obtain the preference pairs.

C Image Classification

C.1 Extensive Results

Table A1 shows the full results of 200 epochs and 600 epochs training on the CIFAR100 dataset using different ViT models. Table A2 shows the three fine-grain datasets, *i.e.*, CUB200, FGVC-Aircrafts, and Stanford-Cars. It is easily found that MergeMix can achieve the SOTA on

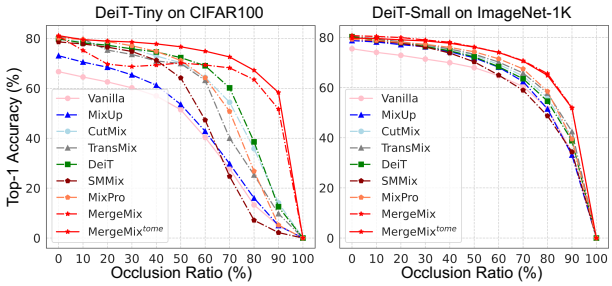

Figure A1: Robustness against image occlusion classification results with different occlusion ratios for different mixup methods based on DeiT-Tiny (left) and DeiT-Small (right) on CIFAR100 and ImageNet-1K datasets.

Table A3: The calibration results of ViT-based mixup methods on CIFAR-100 & ImageNet-1K, with training 200 and 300 epochs respectively. tome denotes inference with token merging.

Models	Dataset	Epochs	MixUp	CutMix	TransMix	DeiT	SMMix	MixPro	MergeMix	MergeMix^{tome}
DeiT-Tiny	CIFAR100	200	8.64	11.42	14.52	12.24	11.80	10.68	7.08	**6.73**
ViT-Small	CIFAR100	200	13.89	14.43	14.22	15.76	12.41	10.65	**9.69**	10.14
ViT-Large	CIFAR100	200	4.76	7.36	16.44	6.71	7.70	6.22	**4.65**	4.70
DeiT-Tiny	CIFAR100	600	6.44	6.01	7.56	8.53	8.35	6.38	**5.45**	5.46
ViT-Small	CIFAR100	600	9.01	6.45	9.12	10.22	9.55	7.42	**5.50**	6.04
DeiT-Small	ImageNet-1K	300	5.66	**4.19**	7.57	8.24	6.53	5.17	6.00	4.52

Table A4: The Top-1 accuracy of DeiT-Tiny trained by various Mixup approaches on the CIFAR100 dataset with different occlusion ratios. tome denotes inference with token merging.

Method	DeiT-Tiny Trained 200 epochs									
	0%	10%	20%	30%	40%	50%	60%	70%	80%	90%
Vanilla	66.68	64.54	62.57	60.20	56.96	51.41	40.32	27.75	13.25	4.99
MixUp	73.06	70.52	68.45	65.39	61.27	53.55	42.80	29.77	16.01	5.01
CutMix	79.58	78.64	77.10	75.83	72.96	70.25	64.40	54.39	35.82	14.08
FMix	77.14	76.01	74.62	73.33	71.27	67.72	63.17	56.18	42.12	17.32
GridMix	76.13	73.79	71.94	69.36	66.36	62.34	56.02	47.30	32.52	14.35
ResizeMix	72.93	71.82	70.53	69.67	67.77	65.22	59.87	50.26	31.26	9.72
SaliencyMix	75.41	74.63	73.57	72.14	69.47	65.05	58.08	44.82	24.14	7.03
Attentive-CutMix	80.27	79.13	77.94	76.98	75.45	71.01	57.75	33.10	12.03	4.02
PuzzleMix	79.97	78.18	77.36	76.04	73.74	70.74	65.83	56.75	40.43	19.41
AutoMix	81.12	78.37	78.40	78.16	77.65	**77.09**	74.63	71.64	67.52	55.61
TransMix	80.66	**79.77**	75.33	73.60	70.98	69.95	63.20	40.02	25.28	9.77
DeiT	79.80	78.20	77.29	75.83	74.59	72.31	69.05	60.18	38.55	12.53
SMMix	78.62	77.78	76.51	74.78	71.25	64.17	47.28	24.72	7.12	2.19
MixPro	80.14	79.61	78.78	77.06	74.81	71.18	64.25	50.75	26.80	5.19
MergeMix	80.88	75.19	69.71	68.72	69.33	70.17	69.36	68.20	63.49	51.72
MergeMix^{tome}	**81.12**	79.49	**78.96**	**78.57**	**77.81**	76.65	**74.89**	**72.58**	**67.24**	**58.32**

lots of models. Also, the speed of overfitting is a significant improvement over other methods, which means the token merge can gather useful information and reduce some redundant tokens.

Table A5: The Top-1 accuracy of ViT-Small trained by various Mixup approaches on the CIFAR100 dataset with different occlusion ratios. tome denotes inference with token merging.

Method	ViT-Samll Trained 200 epochs									
	0%	10%	20%	30%	40%	50%	60%	70%	80%	90%
Vanilla	66.24	62.51	60.37	58.59	56.68	53.61	49.70	39.70	22.60	7.55
MixUp	73.67	71.84	70.80	69.07	66.75	63.52	58.21	48.68	28.72	8.01
CutMix	76.13	73.77	72.93	71.92	70.32	68.32	65.48	59.30	43.11	17.04
FMix	71.27	68.52	66.49	65.78	65.00	62.31	57.80	48.98	30.09	6.19
GridMix	67.99	66.48	65.60	64.21	62.54	60.40	56.98	50.02	34.62	9.74
ResizeMix	66.69	66.90	62.80	58.15	47.00	36.15	36.49	33.07	10.97	2.06
SaliencyMix	73.50	72.12	71.88	71.21	69.97	67.62	63.03	53.12	33.27	11.06
Attentive-CutMix	78.26	72.49	67.52	63.83	60.76	54.93	38.05	27.75	32.20	31.66
PuzzleMix	78.01	76.42	75.54	74.61	73.99	71.46	68.23	63.24	51.51	26.25
AutoMix	77.52	76.74	75.14	72.95	69.71	66.76	62.59	59.00	49.01	27.45
TransMix	78.37	76.29	75.86	75.58	74.79	**73.19**	**70.81**	**68.18**	62.29	51.09
DeiT	77.50	75.99	75.80	74.57	73.80	71.73	67.23	58.40	43.49	19.94
SMMix	79.32	77.84	76.60	75.41	73.00	68.10	58.89	45.07	23.25	4.59
MixPro	79.91	**78.37**	75.36	72.08	68.37	57.48	37.08	21.62	11.87	3.69
MergeMix	81.29	75.38	73.41	69.36	61.02	51.73	52.52	62.14	64.83	57.21
MergeMix^{tome}	**81.66**	77.45	**78.25**	**78.26**	**74.85**	72.02	69.70	67.81	**67.80**	**60.56**

C.2 Robustness Experiments of Mixup Augmentations

Calibration of mixup augmentations Table A3 shows the results of calibration on seven mixup augmentations. We evaluated with two public datasets by DeiT-Tiny, ViT-Small, and ViT-Large on the CIFAR100 dataset, by models trained with 200 epochs, DeiT-Tiny and ViT-Small trained with 600 epochs, and DeiT-Small on the ImageNet-1K dataset, trained with 300 epochs.

Table A6: The Top-1 accuracy of DeiT-Small trained by various Mixup approaches on the ImageNet-1K dataset with different occlusion ratios. tome denotes inference with token merging.

Method	DeiT-Samll Trained 300 epochs									
	0%	10%	20%	30%	40%	50%	60%	70%	80%	90%
Vanilla	75.46	74.03	72.85	71.36	69.91	67.94	64.71	60.42	51.65	34.08
MixUp	78.74	78.17	77.11	76.21	74.31	71.85	68.13	62.40	51.45	33.08
CutMix	80.16	79.23	78.20	76.87	75.21	72.92	69.24	64.63	55.95	39.69
TransMix	**80.36**	79.47	78.24	77.00	75.40	73.31	70.17	65.78	57.79	42.44
DeiT	80.27	79.03	77.92	76.39	74.65	72.25	68.31	63.53	54.57	38.81
SMMix	79.32	78.56	77.70	76.17	73.76	70.25	64.95	58.94	48.69	34.37
MixPro	79.25	78.83	78.01	77.24	76.02	74.26	71.48	67.44	58.49	39.47
MergeMix	**80.70**	**80.38**	**79.95**	**78.97**	**78.08**	**76.21**	**74.08**	**70.71**	**65.57**	**51.98**
MergeMix^{tome}	79.67	**79.57**	**79.01**	**78.60**	**77.68**	**76.11**	**73.99**	**70.56**	**64.84**	**51.80**

Table A7: Classification results of CAFormer small (CAFormer-S12) with different mxiup augmentations, training 200 epochs with 100 batch size on CIFAR100 dataset.

Model	Dataset	Epochs	Vanila	MixUp	CutMix	DeiT	TransMix	MergeMix
CAFormer-S12	CIFAR100	200	74.95	81.64	**84.69**	83.60	83.70	84.30

Results of occlusion robustness The full results of occlusion robustness classification on MergeMix and other mixup methods. Figure A1 shows the curve of MergeMix and other mixup methods on the CIFAR100 dataset and ImageNet-1K dataset. Table A4 and Table A5 show the accuracy results on the CIFAR100 dataset by vanilla and 14 different mixup approaches. Table A6 shows the results of 8 different methods on the ImageNet-1K dataset.

C.3 Further results on different backbone and data modality.

For further exploring the effectiveness of MergeMix, we applied our approach on a hyper-model MetaFormer (CAFormer) (Yu et al., 2022) and two audio datasets for classification by HuBERT-Base (Hsu et al., 2021). ESC-50 (Piczak, 2015) consisted of 50 classes, with 1,200 training samples and 400 validation samples, and a maximum duration of 3 seconds. UrbanSound8k (Salamon et al., 2014) is a classification dataset consisting of 10 classes, with a maximum duration of 4 seconds, containing 7,079 training samples and 816 validation samples. Following the USB experimental setup, we fine-tuned the model for 100 epochs using the AdamW optimizer. The base learning rate was set to `1e-4`, texttt5e-4, with a batch size of 32 and a weight decay coefficient of 5e-4. Both the compared shuffling methods and our proposed MergeMix can be directly transferred to audio data (treated as one-dimensional sequences). Table A8 below shows our reproduced comparison results on two audio datasets. Compared to the MixUp and TransMix baselines, MergeMix achieves significant performance improvements over multiple shuffling baseline models. For CAFormer-S12, we train for 200 epochs on the CIFAR100 dataset with the same settings as DeiT-Tiny. Table A7 shows that MergeMix obtained a second-best result, since CAFormer only has with Attention module of 2 stages (8 layers).

Table A8: Supervised fine-tuning on HuBERT-Base model on ESC-50 and UbranSound8K datasets.

HuBERT-Base	ESC-50	UbranSound8K
Vanilla	75.12±1.07	84.14±0.45
MixUp	75.86±0.83	85.02±0.26
TransMix	76.27±1.14	85.33±0.57
MergeMix	76.51±0.95	85.69±0.42

D VISUAL UNDERSTANDING

D.1 CALIBRATION RESULTS OF MLLM

To explore MLLM calibration, we selected 4 tasks with short responses across different token-reduction settings. We evaluate three scenarios: using full vision tokens, 50% tokens, and 25% tokens, and compare various data augmentation strategies (MixUp, CutMix, ResizeMix, MergeMix) trained with ranking loss (denoted as **rl**). Table A9 shows that with unfreezing the vision encoder, the ECE can be better than freezing. With the vision tokens reduced in training. Overall, token reduction leads to a moderate drop in calibration accuracy, but effective augmentation strategies significantly mitigate this degradation. In the full-token setting, CutMix^{rl} achieves the lowest GQA calibration error (6.09), while ResizeMix^{rl} shows the best SEED result (36.08). When reducing tokens to 50%, CutMix^{rl} and MergeMix^{rl} remain competitive, maintaining strong calibration across tasks despite reduced visual information. Even with 25% tokens, CutMix^{rl} continues to yield relatively balanced performance, indicating that appropriate augmentation enhances robustness under token compression. These results suggest that MLLM calibration remains an open question, especially in environments that require a reliable answer.

Table A9: The calibration results of LLaVA on POPE, ScienceVQA^{I}, GQA & SEED^{I}.

Method	GQA	POPE	SEED^{I}	ScienceVQA^{I}
Baseline	14.57	13.16	33.79	28.09
Training with Full Vision Tokens				
SFT Vision	8.52	12.82	32.67	21.66
+MixUp^{rl}	**6.09**	12.72	33.26	**21.51**
+CutMix^{rl}	6.74	**12.62**	32.77	24.71
+ResizeMix^{rl}	12.53	13.17	36.08	24.58
+MergeMix^{rl}	6.50	12.91	**32.52**	23.66
Training with 50% Vision Tokens				
SFT Vision	18.13	**12.67**	34.41	24.28
+MixUp^{rl}	13.40	12.74	33.60	22.61
+CutMix^{rl}	10.48	12.67	33.83	**20.63**
+ResizeMix^{rl}	12.60	12.97	37.41	23.74
+MergeMix^{rl}	**10.34**	12.76	**33.37**	25.22
Training with 25% Vision Tokens				
SFT Vision	13.32	12.51	34.97	18.86
+MixUp^{rl}	12.97	12.66	34.89	19.33
+CutMix^{rl}	12.23	13.10	**34.85**	20.70
+ResizeMix^{rl}	**10.66**	14.17	38.77	**17.27**
+MergeMix^{rl}	12.55	**12.17**	34.87	17.70

D.2 RELATIONSHIP BETWEEN MIXING RATIOS AND REWARDS

To understand how the proposed ranking loss on synthetic mixed pairs approximates human preference learning, we conduct a `VLM-as-the-judge-eval` evaluation in which strong MLLMs score the mixed pairs generated with different mixing ratios λ. Specifically, we query a diverse set of frontier MLLMs, including Grok-3, Doubao-Seed-1.6 (Guo et al., 2025), Doubao-Seed-1.6-CoT, Qwen3-VL-Plus-32B (Yang et al., 2025a), Qwen2.5-VL-72B (Bai et al., 2025), Gemini-2.5 (Team et al., 2023), and a human-expert baseline, to assign reward scores to each mixed pair. As shown in Figure A2, we found that the reward consistently increases with larger mixing ratios, and this trend holds across nearly all evaluators. The strong monotonic correlation suggests that λ provides a reliable and well-behaved control signal for modeling preference strength. This observation validates our use of λ as an interpretable proxy for preference supervision and highlights its potential as a lightweight alternative to explicit human-annotated reward signals.

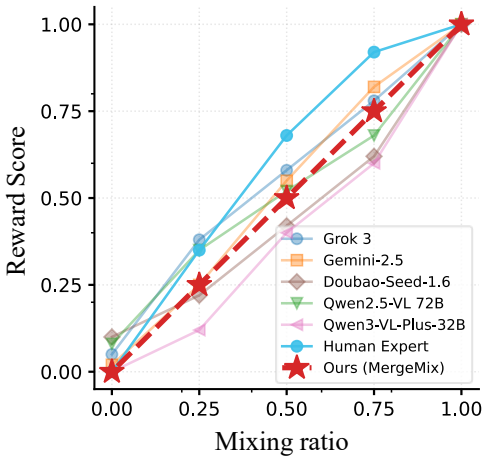

Figure A2: **VLM-as-the-Judge results for different mixing ratios.** Higher mixing ratios consistently yield higher reward scores across strong MLLMs. MergeMix aligns closely with these models, showing that the mixing ratio provides a meaningful preference signal.

Table A10: **Different token merge ratios of inference comparison results with augmentations**. **AVG**: The average of the nine benchmarks for comprehensive comparison, except for MME.

LLaVA-7b v1.5	Train Ratio	Image Question Answering					Benchmarks					AVG	Gain
		VQAv2	GQA	VizWiz	SciVQA^{I}	TextVQA	MME	MMBench	MMBench^{CN}	POPE	SEED^{I}		
Inference Full Vision Token													
Vanilla	–	78.5	62.0	50.0	66.8	58.2	1510.7	64.3	58.3	85.87	66.19	65.57	–
SFT Vision	100%	79.32	62.98	47.45	70.05	57.17	1490.88	66.26	60.05	86.18	67.32	66.31	**+0.74**
+ MixUp	100%	79.27	62.58	44.95	69.41	57.39	1483.20	65.72	58.24	86.27	66.73	65.62	**+0.05**
+ CutMix	100%	79.18	62.40	45.04	70.60	57.06	1452.31	66.32	58.24	86.47	67.22	65.84	**+0.27**
+ ResizeMix	100%	77.78	61.66	44.43	68.91	55.11	1436.09	63.91	55.41	86.01	63.91	64.13	**-1.44**
+ MergeMix	100%	79.24	62.44	47.69	69.86	57.56	1479.97	66.58	60.65	86.10	67.47	66.40	**+0.83**
Inference 75% Vision Token													
Vanilla	–	77.24	59.65	50.86	68.42	55.66	1460.88	63.05	57.9	85.60	65.21	64.84	–
SFT Vision	100%	77.62	59.73	46.57	70.15	54.83	1454.99	65.03	59.36	85.60	65.90	64.98	**+0.14**
+ MixUp	100%	77.66	59.37	44.15	69.91	56.18	1457.98	64.77	57.73	85.15	65.28	64.47	**-0.37**
+ CutMix	100%	77.67	59.21	44.25	69.66	54.84	1400.49	65.03	57.98	85.91	65.66	64.47	**-1.09**
+ ResizeMix	100%	76.45	59.65	43.31	68.82	53.14	1426.75	63.91	55.15	85.29	63.04	63.20	**-1.64**
+ MergeMix	100%	77.71	59.32	47.46	70.70	54.85	1440.50	65.37	58.93	85.04	65.98	65.04	**+0.20**
Inference 50% Vision Token													
Vanilla	–	76.65	59.33	50.45	68.86	55.33	1452.18	62.8	56.87	86.53	64.09	64.55	–
SFT Vision	100%	77.07	59.05	46.19	70.35	54.40	1436.79	64.60	58.93	85.62	65.12	64.59	**+0.04**
+ MixUp	100%	77.11	58.96	44.39	69.36	54.41	1422.28	64.34	57.90	86.16	64.29	64.10	**-0.45**
+ CutMix	100%	77.15	58.66	44.00	69.31	54.78	1428.21	64.94	59.02	86.42	64.80	64.34	**-0.21**
+ ResizeMix	100%	75.90	59.46	42.99	69.31	52.83	1444.13	63.23	54.20	85.77	62.07	62.86	**-1.69**
+ MergeMix	100%	77.13	59.02	47.46	70.55	54.54	1461.63	65.03	58.84	85.70	65.25	64.84	**+0.29**
Inference 25% Vision Token													
Vanilla	–	74.63	58.76	52.71	68.67	55.32	1398.24	60.65	54.03	86.54	62.05	63.71	–
SFT Vision	100%	75.02	58.43	46.36	69.06	52.32	1376.88	62.37	55.84	85.64	63.63	63.19	**-0.52**
+ MixUp	100%	75.45	58.63	44.82	68.02	52.13	1384.31	62.28	60.65	85.54	62.97	63.39	**-0.32**
+ CutMix	100%	75.39	58.61	43.85	68.67	52.69	1330.99	62.71	56.01	86.30	63.02	63.03	**-0.68**
+ ResizeMix	100%	74.08	59.02	43.40	68.96	51.40	1377.96	61.08	53.09	86.53	59.85	61.93	**-1.78**
+ MergeMix	100%	75.50	58.60	48.14	69.86	52.01	1439.44	63.05	57.56	85.53	63.72	63.77	**+0.06**

D.3 Results of Different Vision Token Ratios on Inference

In this subsection, we validate the different ratios of vision tokens on the LLaVA benchmark. Table A10, Table A11 and Table A12 show the fully results with full, 75%, 50% and 25% ratios on inference, respectively. Those results give a full comparison of the influence on the vision tokens. Significantly shown in Table A10, MergMix always brings gains in different merge ratios, from **+0.83** to **+0.06**. Other methods, since they are highly random, cause performance instability.

From the results shown in Table A11, when the training stage uses the token merge, it can achieve an average gain of **66.84%**, which improves **0.43%** over training and inference without token merge training and inference, with an improvement of **+1.27%** than the average performance of the original LLaVA model. Figure A3 shows the average accuracy on the LLaVA benchmark for the LLaVA-v1.5-7B model trained and evaluated under different vision token-merging ratios. The results demonstrate that MergeMix maintains strong performance across a wide range of settings, outperforming or matching other baselines.

D.4 Results of Different Ranking Loss

To understand the effectiveness of ranking loss on preference tuning, we conducted an ablation study for $\mathcal{L}_{\text{SimPo}}^{\text{Mix}}$. Table A13 shows that compared with vanilla SimPO, our approach can bring more improvement.

Table A11: **Different token merge ratios of inference comparison results with augmentations**. **AVG**: The average of the nine benchmarks for comprehensive comparison, except for MME.

LLaVA-7b v1.5	Train Ratio	Image Question Answering					Benchmarks					AVG	Gain
		VQAv2	GQA	VizWiz	SciVQA^{I}	TextVQA	MME	MMBench	MMBench^{CN}	POPE	SEED^{I}		
Inference Full Vision Token													
Vanilla	–	78.5	62.0	50.0	66.8	58.2	1510.7	64.3	58.3	85.87	66.19	65.57	–
SFT Vision	50%	78.6	62.47	48.15	69.51	56.41	1486.24	66.32	57.98	87.37	66.75	65.95	+0.38
+ MixUp	50%	78.51	62.07	51.1	68.47	56.54	1459.06	65.63	59.53	86.86	66.06	66.08	+0.51
+ CutMix	50%	78.58	62.39	50.53	70.2	55.95	1414.72	66.92	59.53	86.56	66.2	66.31	+0.74
+ ResizeMix	50%	76.39	61.05	45.48	68.07	54.60	1447.35	63.31	51.97	86.57	62.54	63.33	-2.24
+ MergeMix	50%	78.61	62.18	52.14	69.61	56.85	1453.97	66.58	59.02	86.47	66.63	66.45	+0.88
Inference 75% Vision Token													
Vanilla	–	77.24	59.65	50.86	68.42	55.66	1460.88	63.05	57.90	85.60	65.21	64.84	–
SFT Vision	50%	78.75	62.82	48.02	70.65	56.33	1486.24	66.40	59.02	86.93	67.17	66.23	+1.39
+ MixUp	50%	78.87	62.32	51.01	69.11	56.62	1480.04	65.63	59.53	86.86	66.06	66.22	+1.38
+ CutMix	50%	78.73	62.42	49.85	70.50	56.12	1418.07	67.61	59.87	85.96	66.44	66.39	+1.55
+ ResizeMix	50%	76.79	61.12	44.85	68.37	54.24	1475.27	64.26	52.66	85.67	63.30	63.47	-1.37
+ MergeMix	50%	78.81	62.50	52.31	69.56	56.51	1455.81	66.66	59.10	85.76	67.12	66.48	+1.64
Inference 50% Vision Token													
Vanilla	–	76.65	59.33	50.45	68.86	55.33	1452.18	62.80	56.87	86.53	64.09	64.55	–
SFT Vision	50%	78.49	63.39	46.69	70.25	55.68	1468.38	66.83	57.76	86.47	66.48	65.78	+1.23
+ MixUp	50%	78.54	61.91	51.01	69.61	55.76	1468.14	65.63	59.87	86.51	66.39	66.14	+1.59
+ CutMix	50%	78.50	62.18	48.79	70.50	55.83	1431.32	67.18	59.02	86.00	66.27	66.03	+1.48
+ ResizeMix	50%	76.55	60.79	44.20	68.32	54.21	1470.22	63.31	52.66	86.23	62.73	63.22	-1.33
+ MergeMix	50%	78.51	62.09	51.01	70.10	56.03	1464.00	66.75	59.45	86.05	66.39	66.26	+1.71
Inference 25% Vision Token													
Vanilla	–	74.63	58.76	52.71	68.67	55.32	1398.24	60.65	54.03	86.54	62.05	63.71	–
SFT Vision	50%	77.30	61.77	46.33	70.55	54.19	1411.01	65.72	58.07	86.34	65.46	65.08	+1.37
+ MixUp	50%	77.28	61.56	48.77	69.56	54.10	1419.71	66.32	56.27	86.57	65.32	65.08	+1.37
+ CutMix	50%	77.20	61.52	49.00	71.24	53.96	1372.66	66.49	58.76	86.38	65.24	65.53	+1.82
+ ResizeMix	50%	75.06	59.88	43.12	67.13	52.34	1445.26	61.51	51.63	86.03	61.59	62.03	-1.68
+ MergeMix	50%	77.20	61.81	51.66	70.35	54.47	1401.58	66.83	59.10	85.92	65.44	66.84	+3.13

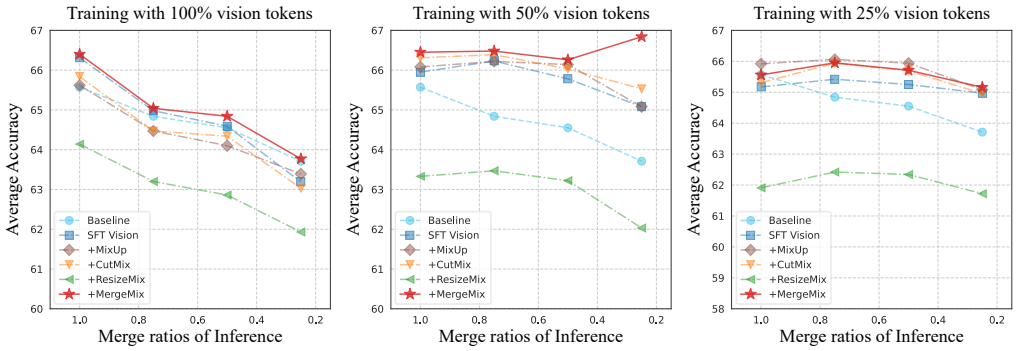

Figure A3: The plots of the LLaVA-v1.5-7B model under different inference time merge ratios for various methods (Baseline, SFT, MixUp, CutMix, ResizeMix, and MergeMix) demonstrate that MergeMix maintains robust performance across a wide range of configurations.

E Efficiency

E.1 Results of Different Vision Token Ratios on Inference

To further validate the inference efficiency gains achieved by Token Merge in MergeMix, we conducted experiments on both image classification models and multi-modal large models. As shown in Table A14, increasing the merging ratio r of the ViT-L model significantly reduces FLOPs (from 59.57G to **34.93**G) while throughput improves from 122.83 to **201.07** (**+63.7%**). Moreover, the

Table A12: Different token merge ratios of inference comparison results with augmentations. **AVG**: The average of the nine benchmarks for comprehensive comparison, except for MME.

LLaVA-7b v1.5	Train Ratio	Image Question Answering					Benchmarks					AVG	Gain
		VQAv2	GQA	VizWiz	SciVQA^{I}	TextVQA	MME	MMBench	MMBench^{CN}	POPE	SEED^{I}		
Inference Full Vision Token													
Vanilla	–	78.5	62.0	50.0	66.8	58.2	1510.7	64.3	58.3	85.87	66.19	65.57	–
SFT Vision	25%	77.92	62.01	50.30	69.11	55.03	1420.69	64.17	56.09	86.82	65.04	65.17	-0.40
+ MixUp	25%	77.89	62.01	52.53	70.20	55.90	1444.45	64.29	57.73	86.94	65.77	65.92	+0.35
+ CutMix	25%	77.92	61.57	51.02	69.21	55.43	1408.18	64.23	57.13	86.09	65.19	65.31	-0.26
+ ResizeMix	25%	75.38	59.77	41.38	66.78	53.45	1430.64	62.37	51.54	85.26	61.26	61.91	-3.66
+ MergeMix	25%	77.86	61.54	50.50	69.56	55.40	1458.49	64.86	57.98	87.22	65.10	65.56	-0.01
Inference 75% Vision Token													
Vanilla	–	77.24	59.65	50.86	68.42	55.66	1460.88	63.05	57.9	85.60	65.21	64.84	–
SFT Vision	25%	78.09	62.11	49.67	69.86	55.03	1423.27	64.94	57.47	85.86	65.77	65.42	+0.58
+ MixUp	25%	77.97	61.23	53.13	69.46	56.17	1466.33	66.06	58.67	86.14	65.67	66.06	+1.22
+ CutMix	25%	78.11	61.85	50.46	69.71	56.08	1420.67	67.52	59.19	85.14	65.42	65.94	+1.1
+ ResizeMix	25%	76.01	59.95	41.94	66.63	53.75	1459.84	63.48	52.92	84.99	62.08	62.42	-2.42
+ MergeMix	25%	78.07	61.42	50.17	70.2	55.96	1483.82	66.58	59.45	86.18	65.49	65.95	+1.11
Inference 50% Vision Token													
Vanilla	–	76.65	59.33	50.45	68.86	55.33	1452.18	62.8	56.87	86.53	64.09	64.55	–
SFT Vision	25%	77.99	61.77	48.79	70.10	54.91	1443.02	64.69	57.38	86.21	65.41	65.25	+0.7
+ MixUp	25%	77.89	61.68	50.85	70.05	56.0	1448.62	66.92	58.07	86.44	65.54	65.94	+1.39
+ CutMix	25%	77.32	61.62	48.86	69.96	55.97	1428.02	67.01	59.02	85.89	65.57	65.69	+1.14
+ ResizeMix	25%	75.78	59.95	40.82	67.33	53.44	1456.66	63.4	53.09	85.57	61.65	62.34	-2.21
+ MergeMix	25%	77.91	61.56	48.86	70.5	56.0	1477.47	66.15	58.76	86.41	65.19	65.71	+1.16
Inference 25% Vision Token													
Vanilla	–	74.63	58.76	52.71	68.67	55.32	1398.24	60.65	54.03	86.54	62.05	63.71	–
SFT Vision	25%	76.97	61.43	49.79	70.0	53.56	1405.86	64.94	56.7	86.81	64.51	64.97	+1.26
+ MixUp	25%	76.84	61.15	49.31	69.66	53.98	1409.16	65.8	57.81	86.72	64.49	65.08	+1.37
+ CutMix	25%	76.89	61.3	48.21	69.32	53.99	1370.27	66.32	57.98	86.42	64.21	64.96	+1.25
+ ResizeMix	25%	75.01	59.72	40.82	66.78	51.66	1418.27	62.45	52.66	85.87	60.54	61.72	-1.99
+ MergeMix	25%	76.91	61.0	48.79	70.2	54.51	1441.07	66.06	58.24	86.57	64.2	65.16	+1.45

Table A13: Ablation study of different ranking loss on LLaVA-v1.5-7B.

Models	SciVQA^{I}	TextVQA	VizWiz	MMBench	Avg.	Gains
LLaVA-v1.5-7B	66.8	58.2	50.0	64.3	59.82	–
mDOP (Wang et al., 2024a)	67.53	57.90	50.04	64.60	60.02	+0.20
Re-Align (Xing et al., 2025)	68.10	**58.55**	**50.06**	64.69	60.35	+0.53
vanilla SimPO	69.86	56.62	49.26	66.24	60.49	+0.67
+ MergeMix	**69.86**	57.56	47.69	**66.58**	61.29	+1.47

additional overhead of Token Merge itself is extremely low (only 0.97 ms at r = 0.75), far below the computational cost of pre-layering. This demonstrates that Token Merge can efficiently compress visual tokens while maintaining negligible overhead. For multi-modal inference, Table A15 shows the effectiveness of Token Merge on LLaVA-v1.5-7B. As r increases, the model's overall throughput improves, while TTFT decreases significantly. The optimal trade-off is achieved at r = 0.5, boosting throughput from 45.96 to **47.28** and reducing TTFT from 86.44 ms to **66.74** ms. When r = 0.75, TTFT further decreases to 62.25 ms. This demonstrates that Token Merge effectively accelerates multi-modal inference without compromising image-text alignment quality. These results collectively show that Token Merge can efficiently reduce the number of visual tokens in MergeMix, thereby lowering FLOPs and inference latency in both visual models and MLLMs. This validates the necessity and advantages of introducing Token Merge into our methodology.

F Visualization and Case Study

In this section, we provide a visualization of the case study of augmentation samples with corresponding performance reward scores and an extensive visualization of mixing samples and ToMe

Table A14: Results of throughput, FLOPs (G), overhead of pre-layer and ToMe by ViT-L model with different merged ratios, evaluated on an Nvidia A100 GPU.

Ratios	Throughput ↑	FLOPs (G)	Overhead Layer	Overhead ToMe
Baseline	122.83	59.57	10.19	–
$r = 0.1$	130.45	56.29	9.82	3.72
$r = 0.25$	145.98	49.37	8.23	3.14
$r = 0.5$	167.54	42.65	5.52	1.79
$r = 0.75$	**201.07**	**34.93**	**3.23**	**0.97**

Table A15: Results of throughput and Time-To-First-Token (TTFT) in ms on LLaVA-v1.5-7B with different merged ratios r, which is evaluated on a Nvidia A100 GPU.

Ratios	Throughput ↑	TTFT (ms)
LLaVA-V1.5	45.96	86.44
$r = 0.1$	43.94	89.32
$r = 0.25$	46.99	83.65
$r = 0.5$	**47.28**	66.74
$r = 0.75$	46.92	**62.25**

source maps. Firstly, we provide a case of different degrees of augmentation in Figure A4. Then, we plot some visualizations of token merge with different merge ratios, mixed samples with different λ in Figure A5 and Figure A6. For every three rows in Figure A5 and Figure A6, the first and second rows of source maps could directly capture the important regions of the raw images, where a large merge ratio enables better grouping of the similar regions. Based on the source maps, when the mixing ratio λ grows from small to large, MergeMix could keep the most distinguishable tokens of the first image while gradually expanding more tokens from less important regions, which enables MergeMix to generate reliable mixing samples with no more computational costs. Moreover, we provide GradCAM (Selvaraju et al., 2019) visualization of the top-1 and top-2 classes with the mixed samples of MergeMix on ImageNet-1K, as shown in Figure A7 and Figure A8.

Figure A4: The visualization of the visual question answers with different mixing ratios by LLaVA-v1.5-7B model. Note that the blue texts denote the core question and the corresponding correct answers, while the green texts denote the wrong answer to the question. The raw image denotes without any augmentations, and other images denote with different mixing ratios λ. Ground-truth Answer denotes the raw labels for this case. With the mixing degree improving, the answer comes out more wrong or unrelated to the question, as shown in green color.

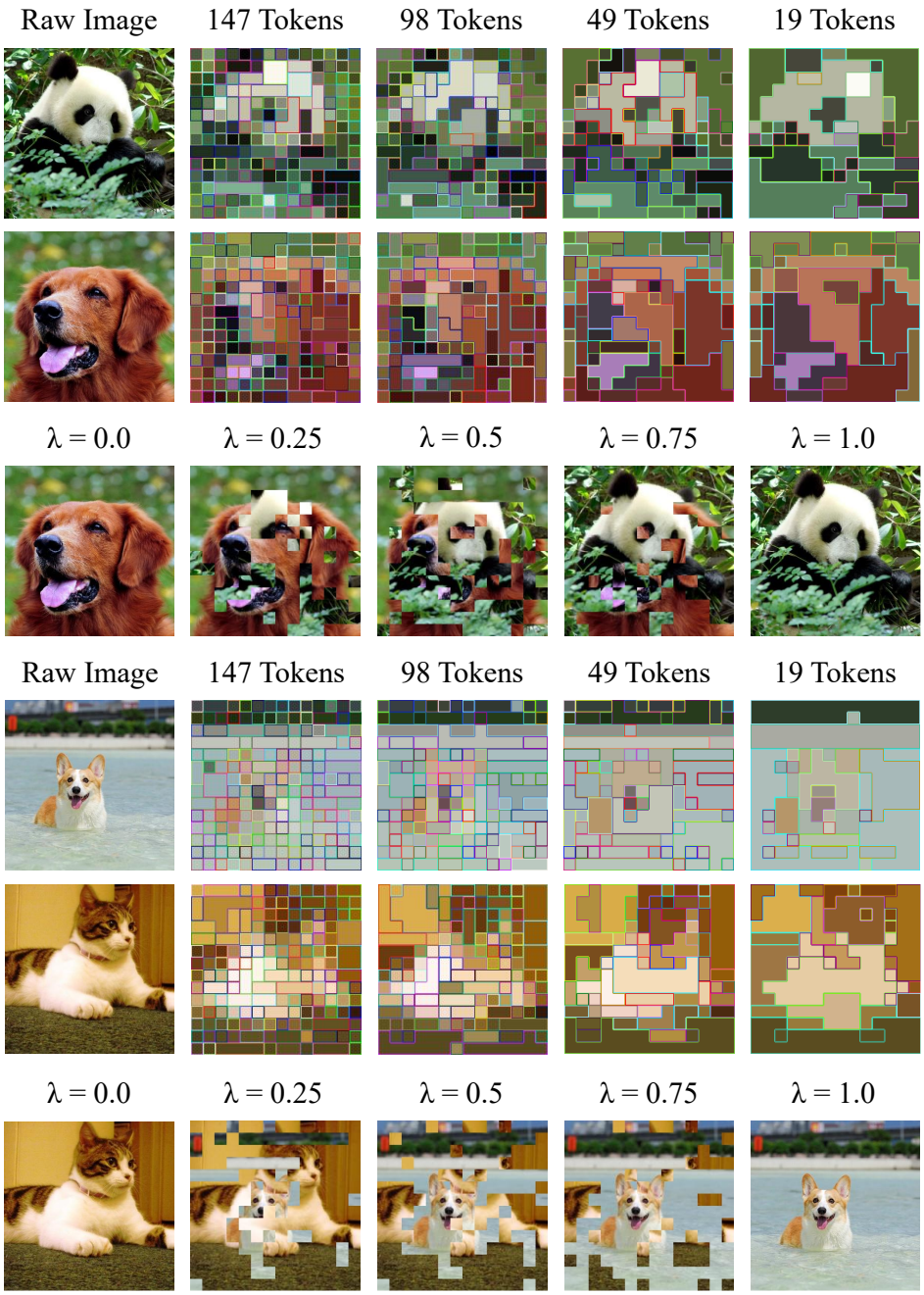

Figure A5: Visualization of mixed samples with source maps of ToMe with different mixing ratios λ and various merge ratios on ImageNet-1K.

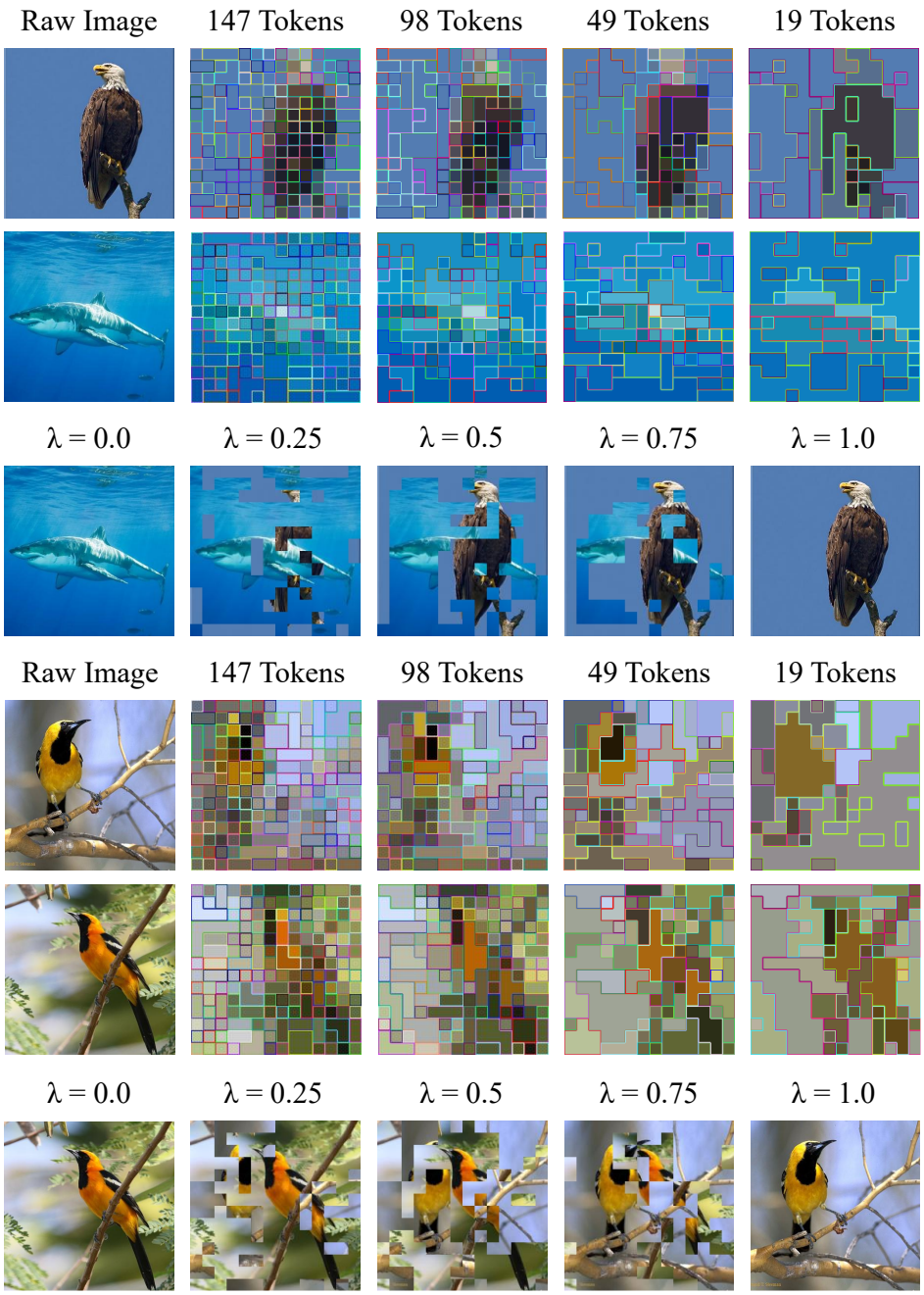

Figure A6: Visualization of mixed samples with source maps of ToMe with different mixing ratios λ and various merge ratios on ImageNet-1K.

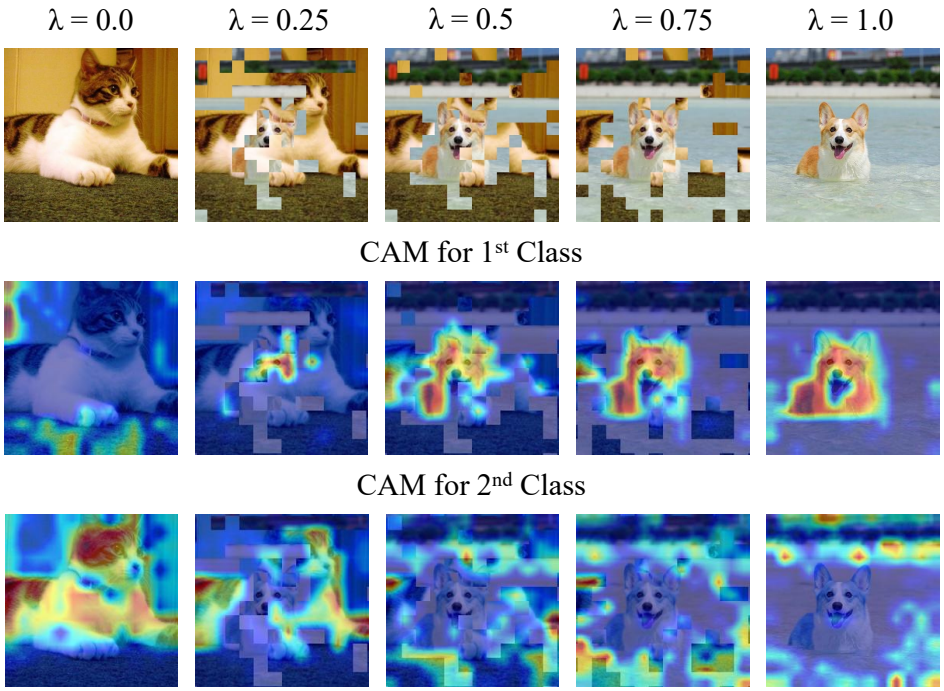

Figure A7: Visualization of mixed samples and corresponding GradCAM (Selvaraju et al., 2019) of the top-1/2 class with MergeMix on ImageNet-1K.

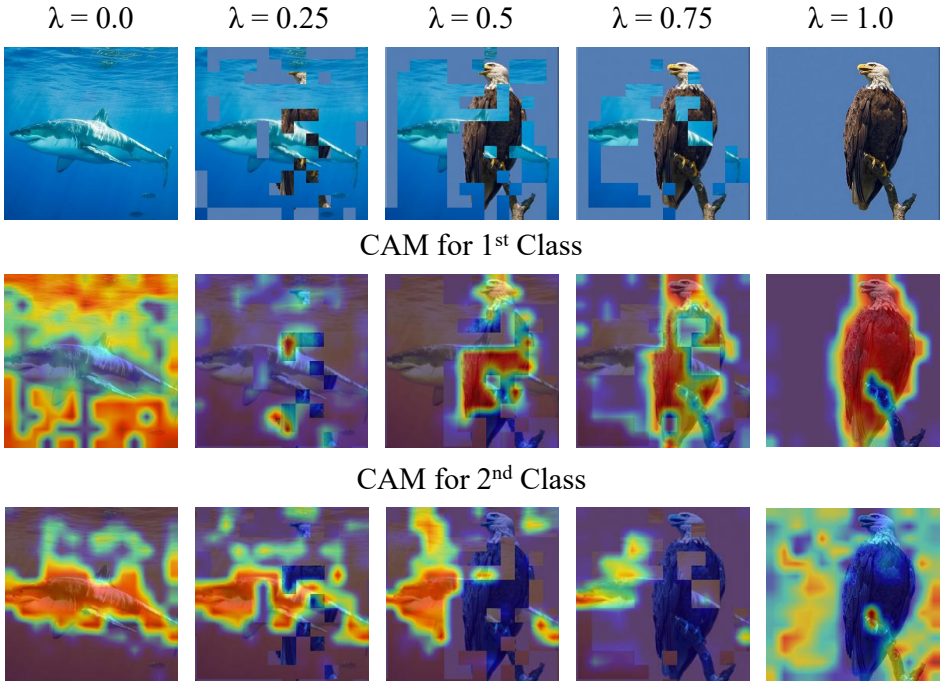

Figure A8: Visualization of mixed samples and corresponding GradCAM (Selvaraju et al., 2019) of the top-1/2 class with MergeMix on ImageNet-1K.